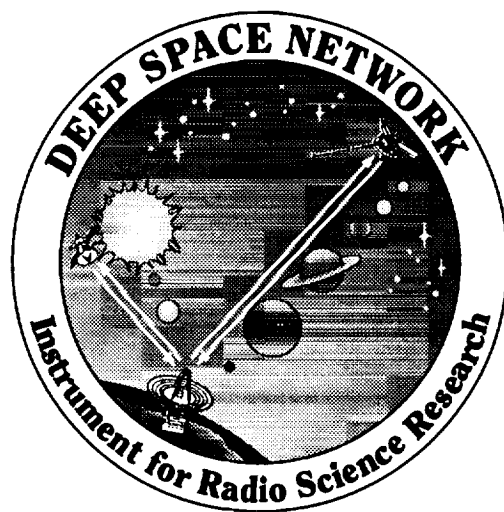JPL Publication 80-93, Rev. 1

The Deep Space Network as an Instrument for Radio Science Research

S. W. Asmar
N. A. Renzetti

April 15, 1993

NASA

National Aeronautics and
Space Administration

Jet Propulsion Laboratory
California Institute of Technology
Pasadena, California

Preface

This document is an update to JPL Document 80-93 dated February 15, 1981. Its two purposes are to present an overview of the accomplishments of the Deep Space Network in the field of radio science research, and to provide to the space science community information on existing as well as currently planned funded Network capabilities. As part of the baseline capability, we have included the implementation being carried out for the Cassini mission to Saturn and Titan. It is planned that future radio science experiments and the anticipated requirements associated with them will be addressed in a separate document by the same authors.

This document has had the benefit of review by members of the radio science community.

Acknowledgements

The authors thank the following individuals for their valuable contributions, comments and suggestions:

Abstract

Radio science experiments use radio links between spacecraft and sensor instrumentation that is implemented in the Deep Space Network. The deep space communication complexes along with the telecommunications subsystem on board the spacecraft constitute the major elements of the radio science instrumentation. Investigators examine small changes in the phase and/or amplitude of the radio signal propagating from a spacecraft to study the atmospheric and ionospheric structure of planets and satellites, planetary gravitational fields, shapes, masses, planetary rings, ephemerides of planets, solar corona, magnetic fields, cometary comae, and such aspects of the theory of general relativity as gravitational waves and gravitational redshift.

Table of Contents

Table of Contents - Continued

I. Introduction

The Deep Space Network is a telecommunications facility managed by the Jet Propulsion Laboratory of the California Institute of Technology for NASA. Its primary function is to provide two-way communications between the Earth and the spacecraft exploring our solar system. To carry out this function, it is instrumented with high-power transmitters, low-noise amplifiers and receivers, and appropriate monitoring and control capabilities. It consists of three complexes situated at approximately equally spaced longitudinal intervals around the globe at Goldstone, California; Robledo near Madrid, Spain; and Tidbinbilla near Canberra, Australia. Two of the complexes are situated in the northern hemisphere while the third is situated in the southern hemisphere. Waff (1993) provides a historical retrospective on the Network's development into the present configuration.

The Network comprises four subnets, each of which contains one antenna at each complex. The four subnets, illustrated in figure 1, are the 70-m diameter subnet (where the stations are designated DSS 14, DSS 43, and DSS 63), the 34-m diameter standard subnet (DSS 12, DSS 42, and DSS 61), the 34-m diameter high-efficiency subnet (DSS 15, DSS 45, and DSS 65), and the 26-m diameter subnet (DSS 16, DSS 46, and DSS 66). Another subnet is currently in the construction phase. It will consist of three 34-m beamwave guide antennas which, in addition to X-band (8.4 GHz) electronics, will also provide efficient communication at Ka-band (32 GHz). It may also transmit at that band to support the Cassini mission radio science experiments.

These deep space communication complexes along with the telecommunications subsystem on board the spacecraft constitute the major elements of the radio science instrumentation. Radio science investigators examine the small changes in the phase and/or amplitude of the radio signal propagating from a spacecraft to an Earth receiving station in order to study the atmospheric and ionospheric structure of planets and satellites, planetary gravitational fields, shapes, masses, planetary rings, ephemerides of planets, solar plasma, magnetic fields, cometary comae, and aspects of the theory of general relativity like gravitational waves and gravitational redshift.
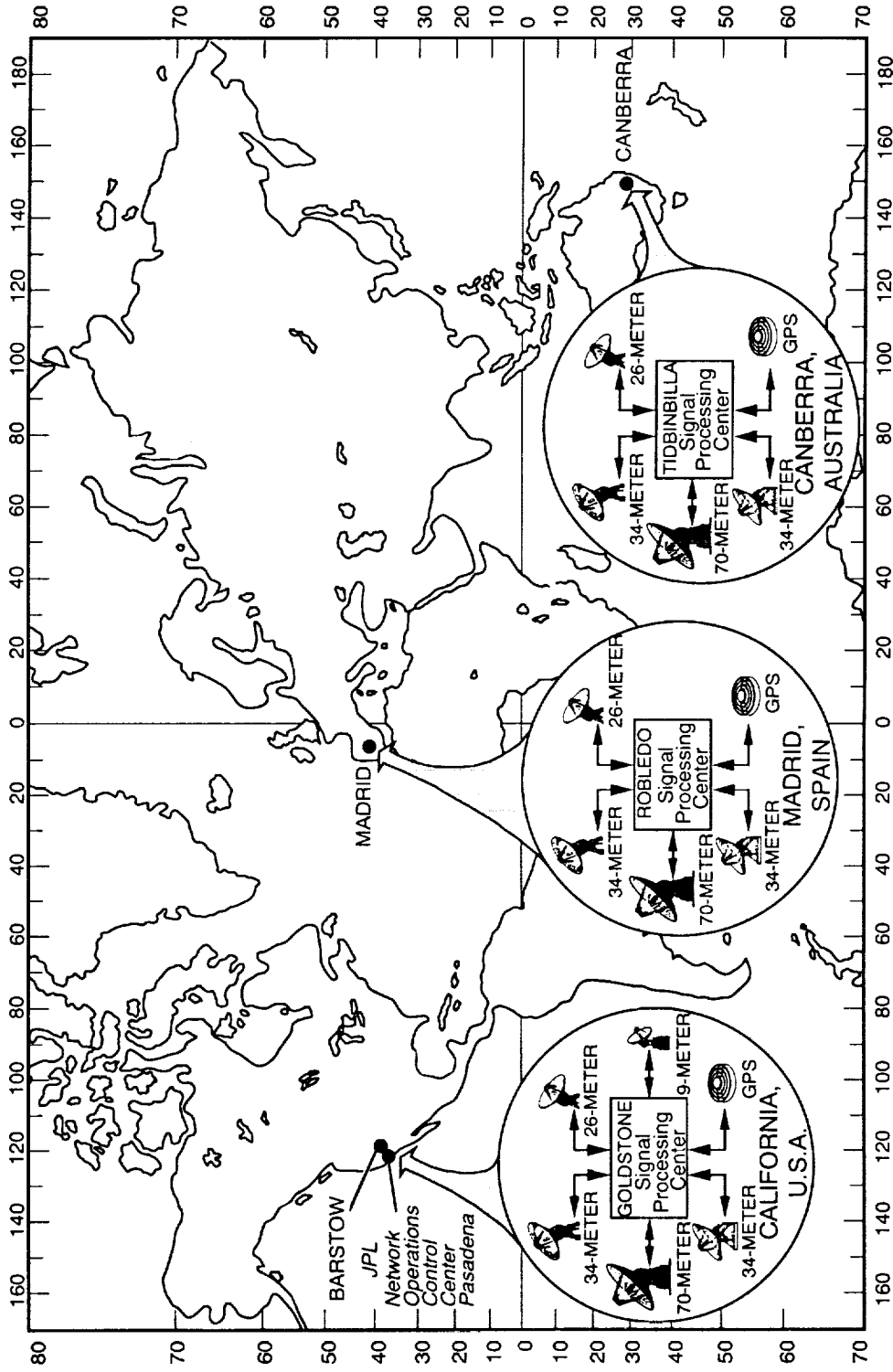
Figure 1. The Deep Space Network 1992 Configuration

2

II. The Network as a Radio Science Instrument

In addition to communicating with the deep space missions, the Network generates accurate radio science data observables. The following is an overview description of the various subsystems at the deep space stations that affect the radio science data. Figures 2 and 3 are block diagrams of these subsystems and illustrate how they interact with each other as well as with a spacecraft radio instrument. Figure 2 shows the example of the Mars Observer mission and figure 3 shows the example of the Galileo mission, without the spacecraft but with additional details of the ground data system. Table 1 lists selected characteristics of the Network's stations applicable to radio science.

The large parabolic surface of the antenna focuses the incoming RF energy onto a subreflector. The subreflector is adjusted in position to optimize the transfer of energy to the rest of the system housed inside the antenna and elsewhere in the complex. In transmission, RF energy is focused on the subreflector which is adjusted to optimize the transfer of energy to the primary reflector and from there to the target spacecraft.

There are several possible ways to keep the massive antennas properly pointed at the spacecraft. One method is "CONSCAN" where the acquired signal is conically scanned by the antenna. The feedback from the closed-loop receiver is provided to an algorithm which compares the scan pattern to the received signal level and compensates to point the scan center at the apparent direction of the spacecraft signal.

In cases of excessive signal dynamics or low received signal levels, as in many occultation experiments, CONSCAN cannot be used and instead the antenna is "blind pointed." Pointing angle predictions are computed for each antenna using an ephemeris provided by the spacecraft navigators. Before the tracking period begins, the predicts are transformed into coordinates for the antenna. An antenna-mounted computer adjusts the coordinates for subreflector position and refraction, and adds a systematic error correction.

With the 70-m and 34-m standard subnets, either of two receiver channels can receive S-band (2.3 GHz) or X-band (8.4 GHz) frequencies. Currently these stations can transmit only at S-band. One

of two circular polarizations is permitted for each frequency band. With the 34-m high-efficiency subnet, only one receiver channel is available and is optimized for X-band frequencies on downlink and uplink (although S-band reception is also permitted). The 34-m antennas have a low-power transmitter (20 kW) available while the 70-m stations also have the high-power transmitter (400 kW).

Once the signal has been focused by the front-end of the antenna, it is channeled to a low-noise amplifier (typically a maser) and then to a receiver. There are two general forms of reception in the Network. One is closed-loop reception which provides, via feedback loop in the circuitry, the capability for rapid acquisition of a spacecraft signal and telemetry lockup. In order to achieve acquisition within the shortest time, the closed-loop receivers may also be predict driven. The carrier signal and ranging spectra are passed to equipment which counts the Doppler cycles and computes the spacecraft range and then transmits the data to JPL in real time. The Doppler and range data types, as well as signal strength information, are processed by the tracking system centered around a metric data assembly and a sequential ranging assembly.

The metric data assembly controls all the tracking system functions at the station. It counts the Doppler cycles and then formats and transmits them to JPL. The ranging assembly measures the round-trip light time of a radio signal traveling from the ground station to the spacecraft and back. As shown in figure 4, a coded signal is modulated onto the carrier and transmitted to the spacecraft where it is detected and transponded back to the station. The received code is then correlated with the transmitted code and the round-trip light-time delay of the signal is measured (see Kinman, 1992, for a review of Doppler tracking of planetary spacecraft). A range observable, r_k, is a measure of round-trip light-time (RTLT) as recorded by the station clock (see Asmar and Kursinski, 1991):

$$r_k = ST(t_k) - ST(t_k - RTLT)$$

where $ST(t_k)$ is the time as kept by the station clock at true time t_k. A Doppler observable, d_k, is defined in terms of differenced range and the Doppler count time:

$$d_k = (r_{k-1} - r_k) / (t_{k+1} - t_k).$$

4

The other type of signal reception is called open-loop. The open-loop receivers do not have a feedback loop with which to track the received signal; instead they rely on frequency predicts to remain tuned to the incoming signal. The signal is downconverted from RF to IF in the antenna and then transmitted to the complex's signal processing center where it is further downconverted to VF. The RF-IF downconverters in the 70-m stations have four IF channels that may be recorded simultaneously. They are the right and left hand circular polarizations of the S- and X-band signals (i.e., XRCP, SRCP, XLCP, and SLCP). The RF-IF downconverters in the 34-m stations have two IF channels: S-band and X-band of either polarization.

A radio science processor digitizes and records the output from the IF-VF downconverters. The data as well as the supporting header information are transmitted to JPL in real time or recorded on magnetic tape at the station. The processor tunes the open-loop receiver based on predicts and allows for frequency and time offsets. It can also snap tune between the coherent and non-coherent frequency channels transmitted by the spacecraft. The radio science instrumentation at the Network also transmits a spectral signal indicator display to the Network Operations Control Center and the Mission Support Area. The displays include the received signal spectra at the station, which are used in real time to validate the radio science system data and monitor the progress of the experiment.

The predicts used for open-loop receiver tuning, closed-loop signal acquisition, as well as antenna pointing are generated by the Network based on the latest trajectory information available for the spacecraft. Models of the planetary atmospheres are also included in the predict-generation software for most of the planets in the solar system. For occultation experiments, it is critical to the process of tuning the open-loop receivers to use predicts with the most accurate atmospheric models and the latest trajectory information available from the mission navigators.

All of the functions necessary to operate and control a complex are centrally located in the monitor and control subsystem. Through this subsystem, the complex receives, stores, and distributes the information needed to operate the stations (e.g., schedules, pointing and tuning predicts). Status information from each subsystem is routed through the monitor and control subsystem to the staff on site and at JPL. Event alarm messages as well as operator logs are processed and displayed through the monitor and control subsystem, where an operator can monitor and control the entire group of equipment (called a link) required to support a given tracking pass.

Several subsystems at the stations require frequency and timing reference. The typical reference is a hydrogen maser standard; cesium standards act as backup. These highly stable clocks are critical to the precision of the radio science data. Current standards provide stability near 10^{-15} at 1000 seconds integration time.

In addition to the radio science data, the Network also makes available ancillary data on the media calibration in the Earth atmosphere. Included are ionospheric calibration data obtained using Earth-orbiting satellites and tropospheric calibration data obtained using surface measurements of pressure, temperature, and relative humidity. Water vapor radiometers may be used in the future.

The Ground Communications Facility supports all the communication requirements of the Deep Space Network including the radio science system. This facility is distributed among different physical locations at JPL and at the complexes. Data lines are used to transmit schedules, sequences of events, and predicts to the complexes from the Network Operations Control Center before a pass, and system status and configuration information from the complex to the operations center during a pass. If necessary, data can also be played back over these data lines at the end of a pass. In real time, the computers of either the radio science support team or the Advanced Multimission Operations System at JPL capture and display all radio science data relevant to the experiments in progress. Voice nets keep the entire operation team in communication by linking the operators at the complexes with the controllers at JPL as well as the project and radio science personnel.

The Radio Science Mission Support Area is the control center for radio science experiments. It is staffed by the flight projects' multi-mission radio science support team for the purposes of conducting operations and monitoring the progress of the experiments. Requirements for configuration for a specific radio science experiment are provided by the radio science support team, representing the flight project and the principal investigators. The configuration typically includes selecting the appropriate stations, open-loop equipment filter bandwidth and sampling rates, antenna pointing method, Doppler sampling rate, and ranging parameters, based on a detailed analysis unique to that experiment (see, for example, Kursinski and Asmar, 1991).

Detailed description of the radio science instrumentation is available in several documents. Interested investigators and engineers are advised, as a starting point, to refer to the latest

revisions of the following JPL documents: Deep Space Network/Flight Project Interface Design Handbook (1988), Deep Space Network/Systems Requirements Detailed Interface Design (1991), and Asmar and Herrera (1993).

Table 1. Selected Characteristics of the Deep Space Stations

	S-band			X-band		
	70-m	3-m STD	34-m HEF	70-m	34-m STD	34-m HEF
Receiving Parameters						
Range of Frequencies (MHz)	2270-2300	2270-2300	2200-2300	8400-8500	8400-8440	8400-8500
Antenna Gain (dBi)	63.3	56.2	56.0	74.2	66.2	68.3
Half-Power Beamwidth (deg)	0.108	0.27	0.24	0.031	0.075	0.063
System Noise Temperature (K)	20	22	38	20	25	20
Polarization(s)	RCP and LCP	RCP or LCP	RCP or LCP	RCP and LCP	RCP or LCP	RCP and LCP
Typical Tracking Loop Noise Bandwidth (Hz)	3-10	3-10	3-12	3-30	3-30	3-48
Transmit Parameters						
Range of Frequencies (MHz)	2110-2120	2025-2120	—	—	—	7145-7190
Antenna Gain (dBi)	62.7	55.2	—	—	—	67.1
Half-Power Beamwidth (deg)	0.119	0.31	—	—	—	0.074
Polarization(s)	RP or LCP	RCP or LCP	—	—	—	RCP or LCP
Transmit Power (kW)	20-400	20	—	—	—	20
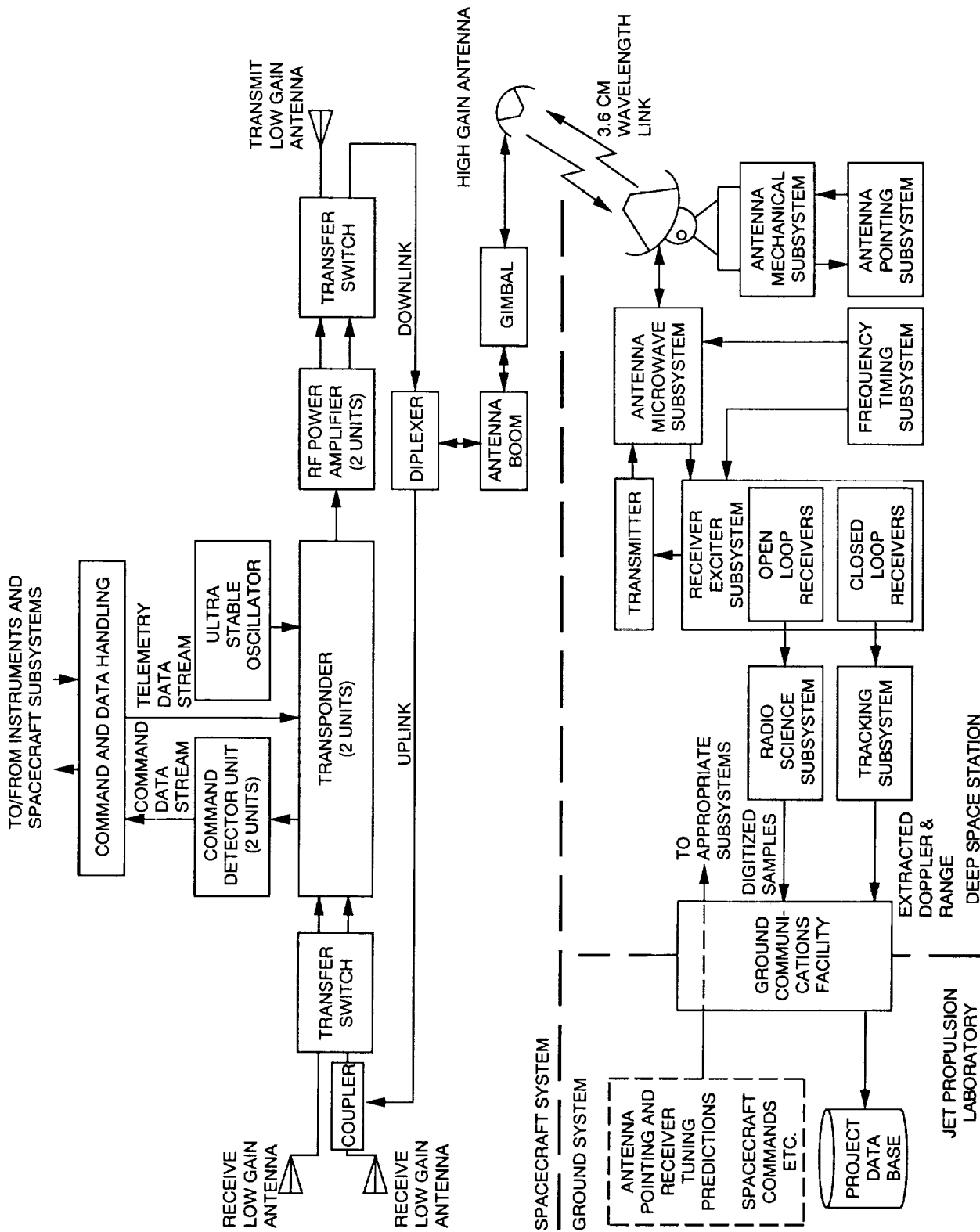
Figure 2. Example of end-to-end radio science instrumentation block diagram for the Mars Observer spacecraft and Deep Space Station
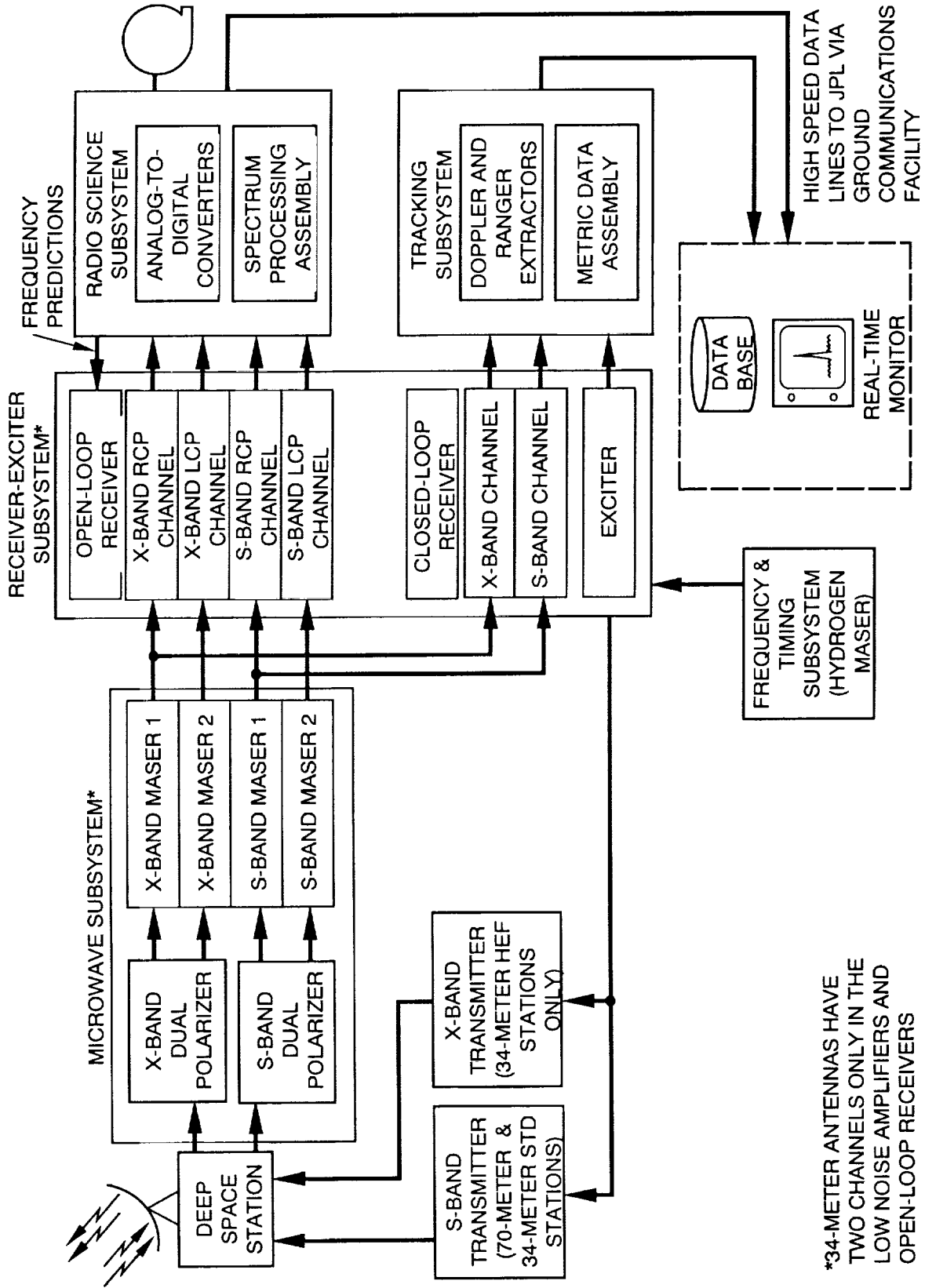
Figure 3. Example of Galileo radio science ground instrumentation block diagram
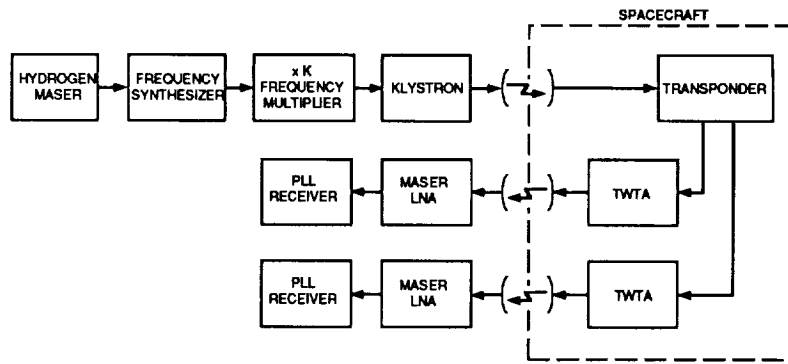
Figure 4a. Two-way coherent Doppler measurement
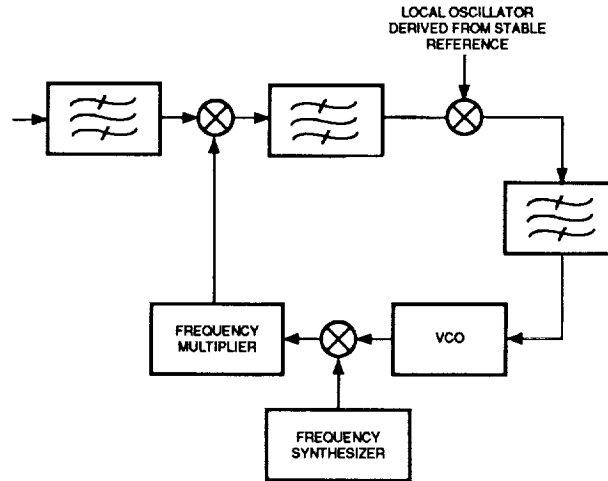
Figure 4b. Phase-locked loop at Deep Space Station
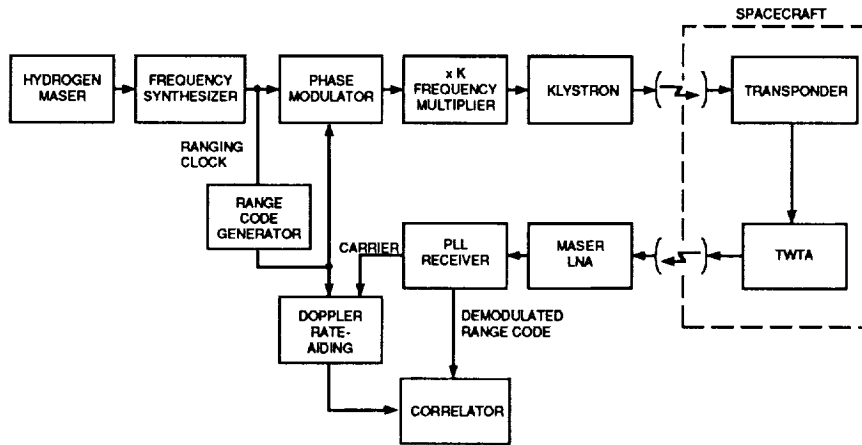
Figure 4c. Range measurement

Figure 4. Doppler and Range Measurements (from Kinman, 1992)

PLL: Phase-locked loop   TWTA: Travelling wave tube amplifier
LNA: Low noise amplifier   VCO: Voltage-controlled oscillator

III. Radio Propagation and Occultation Investigations

Investigations of planetary atmospheres, ionospheres, rings, and magnetic fields using radio propagation techniques have been conducted by almost every planetary mission and are planned for many future ones. In these techniques, radio frequency transmission from a spacecraft occulted by a planet (or one of its satellites) and received on Earth probe the extended atmosphere of a planet. As a result, the radio link is perturbed in phase and amplitude and this perturbation is measured on the ground and converted into an appropriate refractivity profile depending on the object of the investigation. From the refractivity profile, information is derived about the electron distribution in the ionosphere, temperature-pressure profile in the neutral atmosphere, or particle size distribution of the ring material surrounding a planet, in the case of a ring occultation. The refractivity profile is obtained only after the Doppler effect due to the geometrical flight path has been computed and the observed data have been corrected for it. The application of this technique to solar occultations is described in a different section.

The history of radio propagation studies goes back to the early 1960s. Von Eshleman of Stanford University first proposed the method in 1962. Independently, a JPL team led by Dan Cain, conducting a study of the effect of refraction in the Earth's atmosphere on the accuracy of the counted Doppler, realized the possibility of applying the sensitivity of Doppler phase measurements to the study of the atmospheres and ionospheres of other planets (Kliore et al., 1964). The theoretical technique was developed largely by Fjeldbo (1964). The occultation techniques were demonstrated for the first time in 1965 when Mariner IV flew by Mars; they were used to determine the salient features of the Martian atmosphere, showing that the atmosphere is predominantly CO_2 and that the surface pressure is less than one percent of that of Earth, or an order of magnitude less than had been previously believed (Kliore et al., 1965; Fjeldbo and Eshleman, 1968).

A descriptive overview of radio propagation experiments in the outer solar system with the Voyager spacecraft is provided by Eshleman et al. (1977) and Tyler (1987). An overview of Mars Observer radio science experiments is provided by Tyler et al. (1992). The Galileo experiments are described by Howard et al. (1992), and the Ulysses Io plasma torus occultation experiment by Bird et al. (1992c). Mariner, Viking, Pioneer, and Magellan experiments are cited below. Yakovlev (1985) describes radio propagation experiments on Soviet missions.

PRECEDING PAGE BLANK NOT FILMED

PAGE 12 INTENTIO: ALLY BLANK

After the first experiment was performed by the Mariner IV mission to Mars, which provided the first measurement of the Martian surface pressure and temperature as well as a measurement of electron density in the Martian ionosphere, Venus was the next planet probed via radio occultation during the 1967 Mariner V mission (Kliore et al., 1967; Fjeldbo et al., 1971). This experiment also revealed interesting new information about the temperature and pressure profiles in the neutral atmosphere and electron density distribution in the ionosphere. The results of this experiment led to the realization that the Soviet Venera 4 spacecraft did not reach the surface of Venus (Kliore and Cain, 1968; Eshleman et al., 1968).

In order to eliminate the loss of data due to closed-loop receiver lock-up time at the occultation egress and to provide higher stability instrumentation, the Deep Space Network augmented the receiving equipment at the deep space stations with open-loop receivers (see Section II). The new equipment was called the radio science system and has been used by all occultation experiments since the system's implementation.

During the late 1960s and early 1970s, the inner planets continued to be studied by radio scientists. Mariners 6 and 7 flew by Mars (Kliore et al., 1969), then the Mariner 9 orbiter made repeated measurements of Mars (Kliore et al., 1972, 1973); Mariner 10 visited Venus and Mercury (Howard et al., 1974a,b; Fjeldbo et al., 1976). The two Viking Orbiters and Landers provided large amounts of important occultation data during a mission to Mars which began in 1976 and ended in 1982 (Fjeldbo et al., 1977; Lindal et al., 1979).

From December 1979 to October 1992, the Pioneer Venus spacecraft orbited Venus and provided important data on the structure of the ionosphere (Kliore et al., 1979b,c) and atmosphere (Kliore and Patel, 1980; Cimino et al., 1980; Woo et al., 1980), and their changes in response to the solar cycle (Kliore et al., 1991; Kliore and Luhmann, 1991).

In 1973, the Pioneer 10 spacecraft passed by Jupiter, allowing the first occultation measurement of an outer planet. Analysis of these data disclosed the existence of an atmosphere of Io (Kliore and Woiceshyn, 1976; Kliore et al., 1975). In 1974, Jupiter was probed by the Pioneer 11 spacecraft. An occultation experiment was performed during the Pioneer 11 encounter of Saturn, and this experiment yielded the first measurements of the atmosphere and ionosphere of Saturn (Kliore et al., 1980a,b).

14

The Voyager 1 and 2 spacecraft flew by Jupiter in 1979 and Saturn in 1980 and 1981. Voyager 2 also flew by Uranus in 1986 and Neptune in 1989. Some of the findings of the Voyager radio science experiments are summarized below (Tyler, 1987; Tyler et al., 1989). During the Voyager occultations of the atmospheres of the four giant planets, pressure level information was obtained at about 1.0, 1.3, 2.3, and 6.5 bars at Jupiter, Saturn, Uranus, and Neptune, respectively (Lindal, 1992; Tyler et al., 1989). Information can be obtained from these temperature-pressure profiles about the near-adiabatic lapse rates below the tropopause, at about 100 mbar pressure, as well as the considerable structure in the stratosphere. These profiles also provide information on the atmospheric constituents, specifically the ratio of hydrogen to helium. Figure 5 shows the occultation geometries and figure 6 shows the temperature-pressure profiles for the four outer planets encountered by Voyagers 1 and 2. On Neptune, Saturn, and Jupiter, the depth of the measurements was limited by microwave absorption. In the case of Uranus, the depth was limited by the spacecraft trajectory which did not allow link bending angles greater then 3° to be observed. The measurements at Neptune were conducted near 60° north latitude, and the Uranian atmosphere was probed near the equator. The data from Saturn and Jupiter were obtained at latitudes of 36° north and 12° south respectively. The Jovian temperature distribution may have been affected by vertically propagating atmospheric waves (Lindal, 1992).

Voyager also studied the ionospheres of Jupiter, Saturn, and Triton. The ionosphere of Saturn is complex and highly variable with location and time of day. Similar variations with height and location were also reported for Jupiter and appear, from preliminary analysis, to be present on Uranus as well (Tyler, 1987).

Eshleman et al. (1979b) describe the Io torus experiment at Jupiter. Levy et al. (1981) studied the dispersive Doppler measurement of the electron content of the Io torus from the Voyager 1 radio occultation data. Using the occultation data, studies of planetary shapes as well as the magnetic fields of Jupiter and Saturn (Hinson, 1984) were also possible.

The radius of Titan was determined to be 2575 ± 0.5 km during Voyager 1's near-diametric occultation. It was also shown that nitrogen is the major constituent of Titan's atmosphere. The temperature-pressure profile is shown in Lindal et al., 1983; it terminates at a surface temperature of 94 ± 0.7 K. Scintillations were observed at all altitudes below about 100 km, reflecting surprising dynamics in the atmosphere.

The atmospheric radio occultation techniques were extended to planetary ring occultation experiments. During the Voyager 1 encounter of Saturn, the ring occultation experiment led to observations spanning the entire width of the classical ring system. The results are discussed in Tyler (1987); also see publications by Marouf, Rosen, and Gresh in the references. Marouf et al. (1982) describe the theory of ring occultation experiments.

During the Ulysses flyby of Jupiter in February 1992, a path which provided a gravity assist to a polar orbit of the Sun, an occultation experiment was conducted on the Io plasma torus. The spacecraft transmitted signals at 2.3 and 8.4 GHz. The signals were received, recorded, differenced, and integrated in order to derive the columnar electron density of the Io plasma torus (Bird et al., 1992c). The measurements agreed with contemporary models of the torus based on Voyager data, implying that the amount of gas injected from Io is similar to that observed during the Voyager era. On the other hand, the torus seemed to be less extended out in the centrifugal equator, implying a smaller plasma temperature than predicted.

In 1991 and 1992, the Magellan spacecraft also conducted occultation experiments to study the atmosphere of Venus, obtaining highly accurate profiles of atmospheric refractivity and absorptivity (Steffes et al., 1993; Jenkins et al., 1993). These profiles, in turn, provided profiles of ionospheric density, atmospheric temperature, pressure, and sulfuric-acid-vapor abundance. A spacecraft limb-tracking maneuver, plus the high effective isotropic radiated power, made it possible to probe the atmosphere to depths of 35 km at the 3.6 cm wavelength and to 33 km at the 13 cm wavelength.
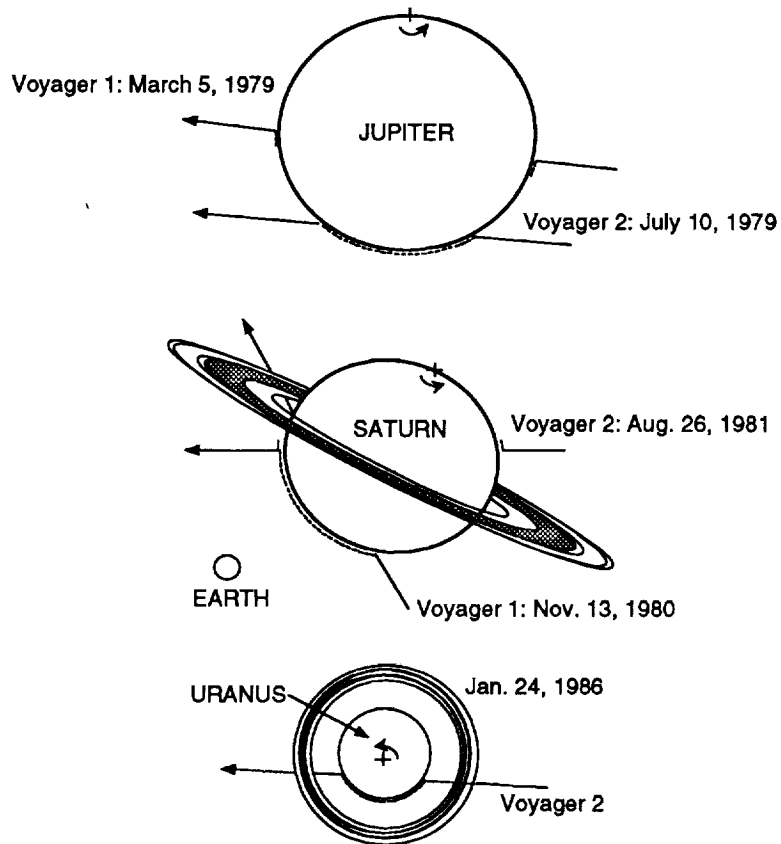
Figure 5a. Voyager occultation geometries at Jupiter, Saturn and Uranus. Figure gives plane-of-sky view of Voyager occultation experiments. Earth is shown to scale (from Tyler, 1987)
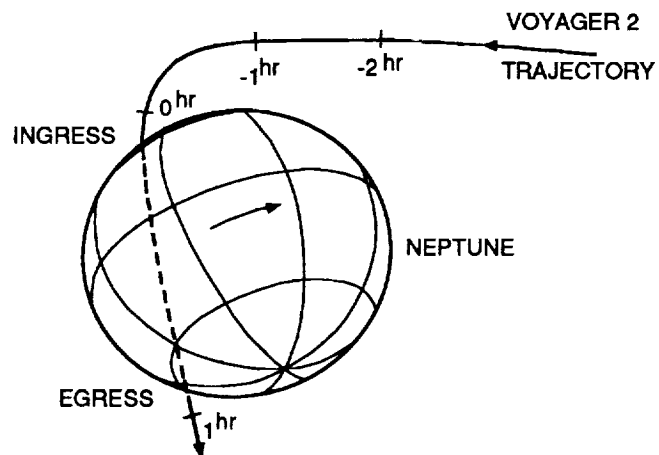
Figure 5b. View from Earth of Voyager occultation of Neptune (from Lindal, 1992)

Figure 5. Voyager occultation geometries
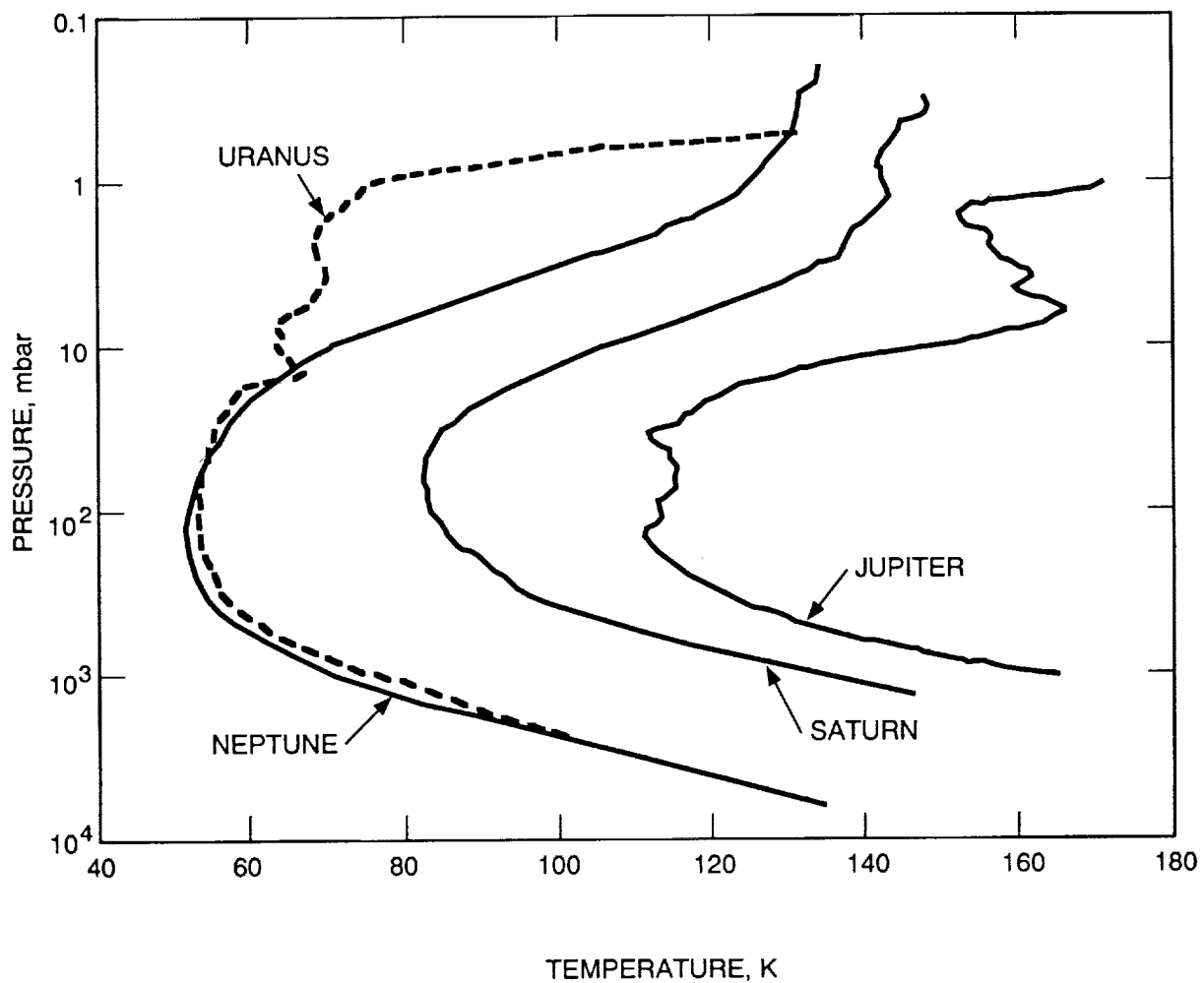
Figure 6. Temperature profiles for the giant planets derived from radio occultation data acquired with the Voyager spacecraft (from Lindal, 1992)

IV. Solar Corona and Solar Wind Research

An overview of radio sounding techniques for studies of the solar corona has been recently presented by Bird and Edenhofer (1990). The first use of the Deep Space Network in solar coronal research consisted of a spectral broadening experiment performed by Goldstein (1967) as the Mariner 4 signal passed within 0.6 deg of the solar disk. Goldstein and colleagues used the not yet completed Goldstone 64-m station to receive the very weak Mariner 4 signals (weak because the spacecraft antenna was not pointed at Earth) via an open-loop receiver driven by an oscillator programmed with the predicted spacecraft received frequency profile. The 100 kW uplink was provided by the Goldstone 26-m antenna. In 1968, Goldstein (1969) duplicated the experiment with the superior conjunction of Pioneer 6 and obtained results similar to those from the Mariner 4 experiment. The radially dependent spectral broadening obtained by Goldstein and colleagues reflected the now better understood relationship between spectral broadening and integrated coronal electron density.

More recently, Woo (1978) obtained extensive near-Sun spectral broadening measurements of the Helios 1 and 2 spacecraft, and used these data in an examination of spectral broadening. A substantial set of Helios and Pioneer spectral broadening data has been empirically compared to an electron density (N_e) model of the following form, where r is the radial distance and A and B are fit constants:

$$N_e = Ar^{-6} + Br^{-2.3}$$

For spacecraft near solar conjunction, range measurements as a function of solar offset distance provide an excellent method of mapping electron density in the solar corona, provided all other competing effects, such as trajectory errors, unmodeled spacecraft forces, and relativistic effects can be properly accounted for. Muhleman et al. (1971) first used this method during the solar conjunctions of Mariners 6 and 7. Using ranging data acquired at the Goldstone 64-m station, Muhleman and colleagues (Muhleman et al., 1977) were able to model the coronal electron density as

$$N_e = Ar^{-6} + Br^{-\varepsilon}$$

where ε = 2.05 for Mariner 6, and 2.08 for Mariner 7, a functional form which is in good agreement with earlier eclipse measurements. A similar experiment was performed some years later using Helios, which produced results consistent with those of Mariners 6 and 7. Bird and Edenhofer (1990) summarized in figure 7 the work of various investigations on the solar wind velocity as a function of solar distance.

The effect of columnar charged particles on the group velocity of electromagnetic waves is given by Koehler (1968) as

$$r = Kf^{-2} \int N_e dR$$

where

        r = observed range delay, m
        K = 40.3
        f = carrier frequency, Hz
        N_e = electron density, m^{-3}
        R = signal path, m

Another radio sounding experiment was performed in November 1968, when the Pioneer 6 spacecraft was occulted by the Sun. Pioneer 6 transmitted a linearly polarized carrier, which allowed the first experiment to be performed using a human-made signal source to determine the Faraday rotation of the solar corona (Stelzried, 1970). The quasi-longitudinal approximation for Faraday rotation is given by (Stelzried et al., 1970):

$$\Omega = Qf^{-2} \int N_e B_L dR$$

where

        Ω = Faraday rotation, deg
        f = signal carrier frequency, Hz
        Q = 1.3548 × 10^6
        R = signal path, m
        N_e = electron density, m^{-3}
        B_L = longitudinal component of solar magnetic field, T

Measurement of coronal Faraday rotation, therefore, provides information about both electron

density and the solar magnetic field (Rusch and Stelzried, 1972). To support this experiment, the Goldstone 64-m station was equipped with a remotely rotatable, microwave linear feed (Reid et al., 1973). A closed-loop polarimeter (Ohlson et al., 1974) was implemented and used to automatically track the orientation of the received signal polarization. This system maximized the received signal strength and yielded precise signal polarization data. Observations during November-December 1968 yielded information on both solar coronal transient events (Levy et al., 1969) and the background solar corona. Research using the polarization tracking capability at the Network's three 64-m stations (now 70-m stations) was continued with the Pioneer and, especially, the Helios spacecraft (Volland et al., 1977; Bird et al., 1977). The Helios Faraday rotation data were also used in studies of the magnetic field in coronal mass ejections (Bird et al., 1985) and the mean background coronal field during solar minimum conditions in 1975-76 (Pätzold et al., 1987). Dennison et al. (1978) made further use of these results with a measurement of the gravitational deflection of a polarized signal propagating through the solar corona. Another Faraday rotation experiment was conducted with the Magellan spacecraft in 1992. Figure 8 from Howard et al. (1992) shows coronal Faraday rotation data recorded simultaneously at widely separated Deep Space Stations.

Using single frequency (S-band) Doppler data acquired during the 1975 solar conjunctions of Pioneer 10, Pioneer 11, and Helios 1, Berman and Wackley (1976) demonstrated that the observed Doppler fluctuations provide an excellent measure of solar wind turbulence. This was significant in that Doppler noise was already being automatically recorded for purposes of ground tracking system performance monitoring, and hence represented a free source of scientific data for coronal studies. Using this data type, it was demonstrated (Berman et al., 1981) that the mean level of Doppler fluctuations is proportional to integrated electron density.

A far more powerful tool for measuring electron density is available when dual-frequency carriers are transmitted from a spacecraft. In this case, differenced range measurements made at the two frequencies provide a direct measurement of columnar electron density that is not contaminated with the multitude of other factors previously mentioned. The Viking spacecraft were equipped with this dual-frequency capability, and the 1976-77 and 1978-79 Viking solar conjunctions provided excellent electron density measurements (Tyler et al., 1977; Muhleman and Anderson, 1981). Dual-frequency ranging observations acquired during solar occultations of the Voyager spacecraft in 1985 and 1988 were reported by Anderson et al. (1987) and Krisher et al. (1991) respectively. Kinman and Asmar (1988) used the 1985 Voyager 2 solar conjunction to study the

two-way coherent Doppler error due to the solar corona inducing phase scintillations on the uplink.

Utilizing dual-frequency (S-band minus X-band) Doppler data from the Mariner 10 spacecraft, Woo et al. (1977) demonstrated that the columnar phase fluctuation spectral index was approximately -2.6:

$$W_o(\nu) \propto \nu^{-2.6}$$

where

W_o = columnar phase spectral density, rad^2/Hz

ν = fluctuation frequency, Hz

This work made a significant contribution to the gradual resolution of the controversy about the value of the spectral index, which originated in the early days of (natural source) interplanetary scintillation observations. More recently, Woo and Armstrong (1979) have studied the variation of the spectral index with radial distance using Viking solar conjunction data and have concluded that a significant change occurs in the spectral index at a solar offset distance of approximately 20 solar radii.

In addition to the radial dependence of Doppler noise, the highly dynamic solar wind causes temporal variations in Doppler noise. Statistical studies show that the occurrence of Doppler noise transients depends strongly on the phase of the solar cycle. While the rate of the transients is about one every four days during solar maximum conditions, it drops by a factor of 3 to 4 during solar minimum (Woo, 1988; Armstrong et al., 1992). Comparison of Doppler noise with in situ plasma measurements indicates that most of the transients are interplanetary shocks during solar maximum (Woo and Schwenn, 1991), while during solar minimum, some of the transients are corotating high speed streams (Woo and Armstrong, 1992). Examples of this comparison are reproduced in figure 9, showing the time histories of Helios 1 in situ measurements of proton temperature T_p, proton density n_p, proton mass flux density $n_p v_p$, and Pioneer Venus rms Doppler scintillation σ_D during April 23-28, 1981. The three Doppler transients T2, T3, and T4 detected by Pioneer Venus at 15 to 18 solar radii were observed later at 170 to 174 solar radii by Helios 1 as shocks S2, S3, and S4, respectively.

The intensity of the Doppler noise transients, as characterized by the enhancement above a background Doppler noise level, is proportional to, and hence indicative of, the speed of the

interplanetary shock. The largest transients seem to represent the fastest shocks, which decelerate strongly while propagating away from the Sun, and are associated with flares (Woo and Armstrong, 1981; Woo et al., 1985; Woo, 1988). On the other hand, the smaller transients seem to represent shocks with relatively low speeds. These move uniformly through the interplanetary medium and are more often associated with the eruption and ejection of cool filamentary material from coronal quiescent regions (Woo et al., 1990).
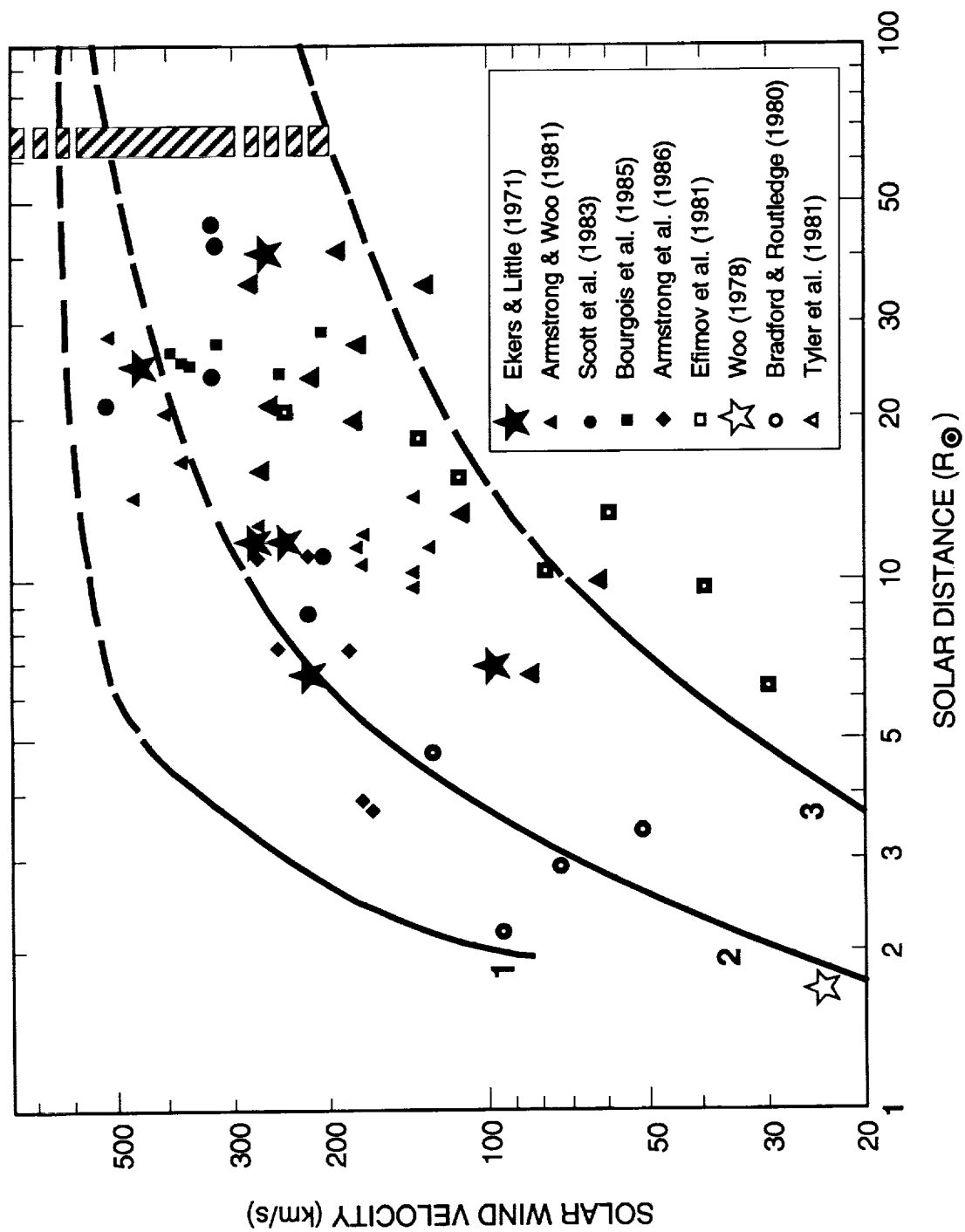
Figure 7. Summary of various investigations of the solar wind velocity as a function of solar distances (from Bird and Edenhofer, 1990)
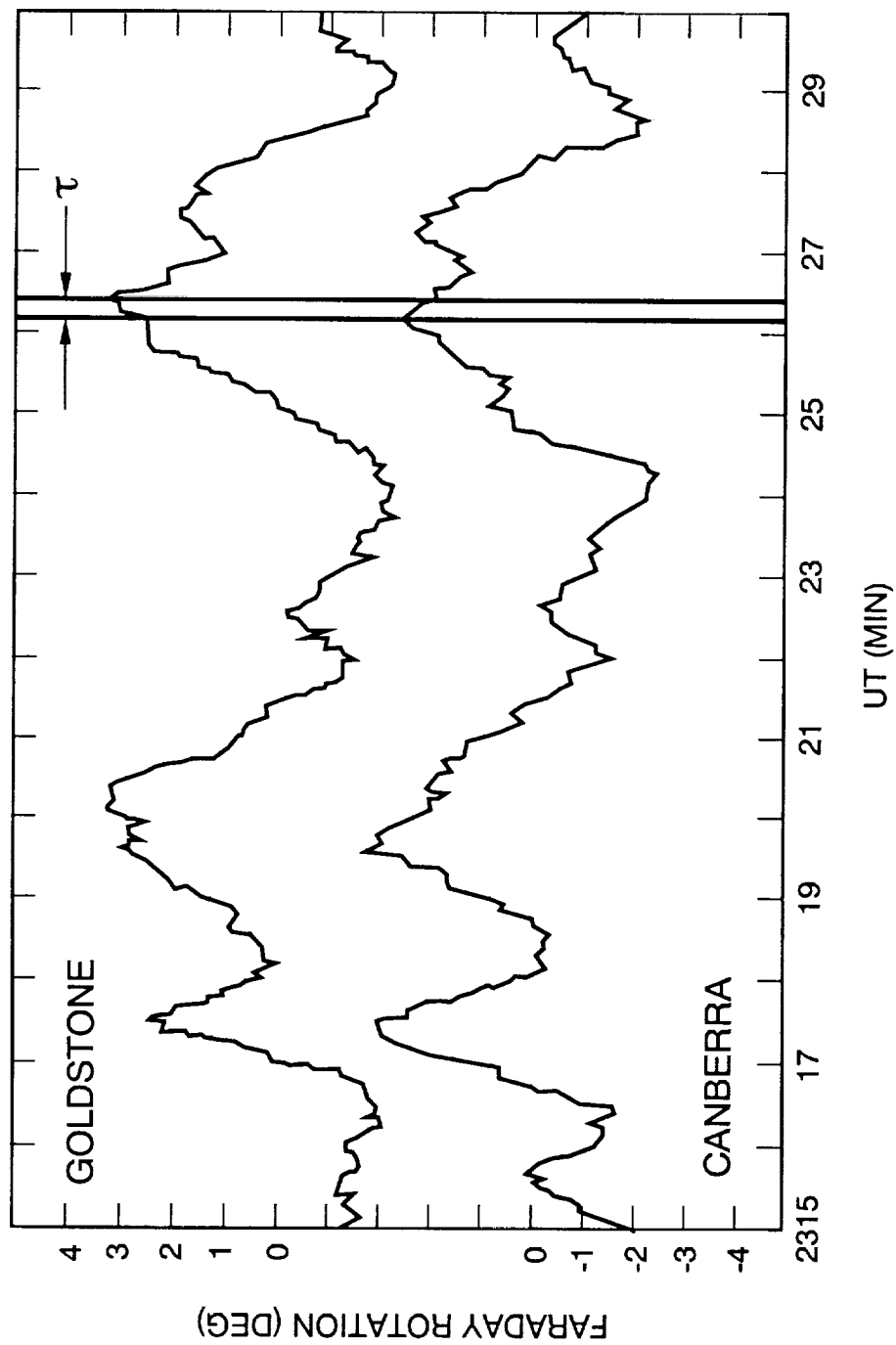
24

Figure 8. Faraday rotation data recorded simultaneously at widely separated Deep Space Stations (from Howard et al., 1992)
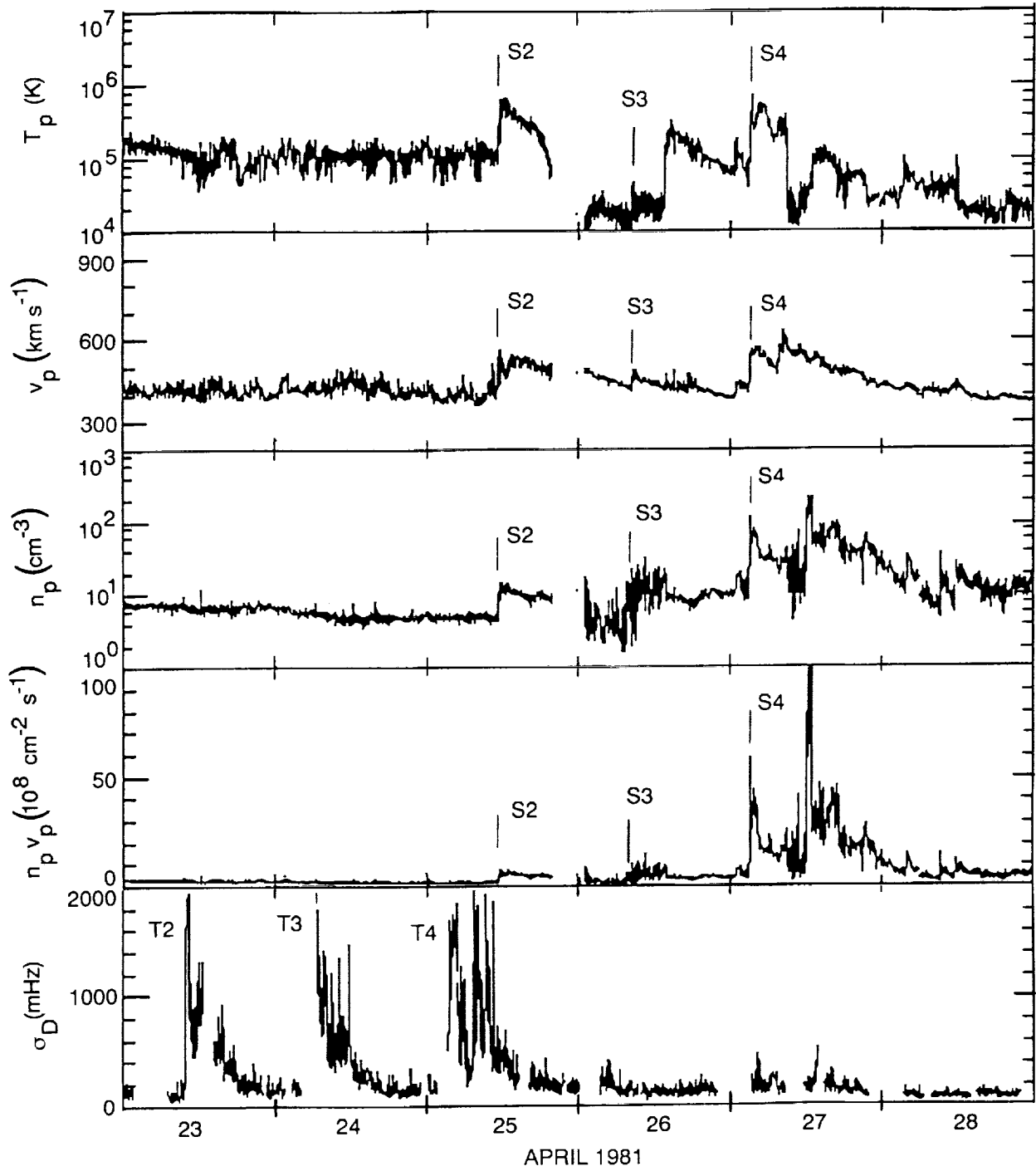
Figure 9. Time histories of Helios 1 in situ data (top 4 panels) and Pioneer Venus
Doppler scintillation data (bottom panel) showing same features; see text
(from Woo and Schwenn, 1991)

V. Celestial Mechanics Investigations

Perhaps the earliest radio science application of Deep Space Network capabilities occurred in the area of celestial mechanics. Previous to the era of deep space exploration, calculation of the physical properties of the planets (mass, size, shape, and orbit) had to be conducted via remote optical astronomical techniques. The ability to make accurate distance and velocity measurements of the deep space probes that were perturbed by a planet's gravitational field allowed in situ measurements of planetary constants for the first time. Gravitational properties of the planet's satellites can also be determined. In the large planet/satellite systems like Jupiter and Uranus, for example, satellites can create motions of the planet which then produce a detectable effect on the spacecraft.

A fundamental property of a planet is its gravitational field, which encompasses many aspects of a planet's composition and motion. This field is represented by an nth degree and order (D&O) two-dimensional spherical harmonic series. The planetary mass scales the harmonics of the field. The ratio of the Sun's mass to the mass of a planetary system is an important celestial mechanics parameter, used in calculating the ephemerides of planetary bodies. Additional lower degree terms in a field describe the dynamic oblateness and the rotational axis, as well as place constants on the deep interior structure of a body. Higher degree terms describe in increasing detail shallow and/or localized gravity features of the planet's surface, including mountains and craters.

Knowledge of a gravitational field, along with a determination of the surface topography and the planet's volume (achieved through optical imaging, radio science occultations, or onboard spacecraft altimeters), produces the mean density of a planet. The information about the internal structure of the planet, when combined with an optical or radar map of surface features, can place constraints on models describing the differentiation of interior layers and the chemical composition and physical state of the interior. In turn, these models can be used in arguments for different theories of solar system evolution. For example, different ideas on satellite origins or planetary condensation can be strengthened or ruled out based on the abundance of certain materials in moons or asteroids.

The use of radio science in celestial mechanics experiments began with the 1962 Mariner 2

mission to Venus and the 1962 Ranger mission to the Moon. Using the Network-generated Doppler navigation data from the Mariner mission, Anderson and Warner (1966) were able to make order-of-magnitude improvements over the previous, earthbound, determinations of the masses of the Moon and Venus. With the Ranger mission, estimates were made of the masses of the Moon and Earth and an estimate was made of the offset between the lunar center of gravity and center of figure. Subsequently, Mariner 4 (Mars), Mariner 5 (Venus), and Mariner 9 (Mars) provided the mass and first estimates of low order gravitational harmonics for Venus and Mars, respectively (see Anderson, 1974, for a review), while analysis of Doppler measurements from the Lunar Orbiter and Apollo missions led to the discovery of large positive gravity anomalies ("mascons" for mass concentration) on the Moon (Muller and Sjogren, 1968).

Mercury was also observed during this period, by two Mariner 10 flybys (1974 and 1975). Analysis of the data yielded the mass and dynamical oblateness of Mercury (Esposito et al., 1978; Howard et al., 1974a). A recent re-analysis of the same data has produced a mass accurate to 0.4%, second order coefficients of the gravity field, and identification of a gravity anomaly in the vicinity of the spacecraft's closest approach point (Anderson et al., 1986a).

Venus has received intense scrutiny in the time since the first Mariners. The data volume from the long-term orbiting spacecraft was equivalent to thousands of single flybys. Most notably, the Pioneer Venus Orbiter, in operation since 1979, and the Magellan radar mapper, in orbit since 1990, have produced a wealth of information, making the Venus gravity field the best known planetary field after the Earth's, and many studies have been made using the data from this period. The Pioneer Venus Orbiter and Magellan data have been combined in at least one study, producing a 60th degree and order spherical harmonic gravity model and 120th degree and order spherical harmonic topography model, which are the most accurate to date (Konopliv et al., 1993). Previous studies have produced estimates of fields to 50th degree and order, using only Pioneer Venus Orbiter data (Nerem et al., 1993).

Various gravity anomalies have also been identified on Venus. These features of the gravity field are especially interesting because the topography of Venus has been mapped with such high accuracy. Correlating the gravity and topography data sets provides invaluable information on the dynamics of the Venusian crust. Areas having received particular attention include the Ishtar Terra plateau (Sjogren et al., 1984), the Beta and Atla Regions (Sjogren et al., 1983), and Aphrodite Terra (Black et al., 1988), with many other regions also explored (for examples see

28

Smreker and Phillips, 1991).

Changing orbital characteristics of these spacecraft, including periapsis, latitude, and eccentricity, allow new features of the planet and its gravity field to be identified and allow different perspectives on old information. Magellan has suspended radar mapping and, in September 1992, lowered its periapsis altitude to 182 km for a Venus gravity campaign, which is expected to last until May 1993. At that time, aerobraking will result in circularization of the orbit for additional gravity coverage.

Mars has also had the benefit of orbiting spacecraft, with the start of the Mariner 9 orbit in 1971 and the two Viking orbiters arriving in 1976. The best gravity model is a 50th degree and order field (Nerem et al., 1993); its best resolution is near the equator due to the large eccentricities of the orbiters and periapsis latitude being nearly equatorial. So the poles, for example, are hardly characterized at all. As with Venus, Mars data have exhibited many interesting gravity anomalies, whose corresponding surface features have been recorded by the Viking cameras. These features include Olympus Mons, which is the largest known gravity anomaly in the solar system (see figures 10 and 11), the mascons in the Isidis basin (Sjogren, 1979), the Hellas Planitia gravity low (Sjogren and Wimberly, 1981), and the Tharsis region (Janle and Erkul, 1991).

Mars will receive its closest scrutiny starting in October of 1993, when the Mars Observer spacecraft arrives. Mars Observer has both a high-resolution camera (2.8 km feature resolution) and altimeter (30-m resolution) for surface characterization, and radio science gravity campaigns will be performed throughout the approximately 2-year mapping cycle. It is expected that from a 50th to perhaps a 70th degree and order global field will be produced. Because of the nearly circular, low altitude (378 km) orbit and polar inclination of the spacecraft, the Mars Observer radio science team expects that the Mars gravity field will eventually be known more accurately than even that of the Earth. Discussions of gravity results from previous Mars missions as well as predicted Mars Observer contributions to Mars gravity field knowledge appear in Rosborough and Lemoine, 1991, and Tyler et al., 1992.

Until the arrival of the Galileo spacecraft in 1995, Jupiter will have had only spacecraft flybys for gravity field investigations. Pioneers 10 and 11 both passed by the planet, closer in fact than the later Voyager 1 and 2 encounters. Data from all four flybys were combined in one study (Campbell and Synnott, 1985), and allowed mass calculations for the four Galilean satellites that

were a factor of 12 better than the analysis of Pioneer data alone. Even the combination of all the data was not sufficient to produce any harmonic terms for the satellite fields. Jupiter mass was determined to 0.00008%, and estimates of several of the low even harmonic coefficients were obtained (see Anderson et al., 1992c, for review). No features of the inner core of Jupiter or any other gas giant planet have ever been observed.

The Galileo Orbiter is not expected to significantly increase understanding of the Jupiter gravity field, as its orbit will remain at a much higher altitude than that of any of the flyby missions. However, a great deal of new knowledge will be obtained regarding the larger satellites and the rotational and tidal characteristics of their interaction. For example, encounters with Io and Ganymede are expected to provide enough information to make decisions possible among different chemical and physical composition models (Anderson et al., 1992c).

Both Voyagers (1980 and 1981), along with Pioneer 11, also made flybys of Saturn. Though Pioneer 11 flew closer to the planet, proximity of the ray path to the Sun introduced a large amount of plasma noise in the signal, and Voyager data were therefore an improvement (Null et al., 1981 for Pioneer results). The Voyagers also obtained closer looks at some of the larger Saturnian moons. A study combining the Voyager and Pioneer data was produced by Campbell and Anderson (1989), which also contains descriptions of previous results for Saturn gravitational characteristics. In it are improved masses for the moons Rhea, Titan, Tethys, and Iapetus, as well as several harmonic coefficients of Saturn's gravity field. In addition, upper limits on second-order coefficients of Titan's gravity field were also calculated.

One small moon, 1981 S13, was first detected with the Voyager 2 Network-generated Doppler data. After gravitational perturbations were noticed in the spacecraft's motion, optical images of candidate body locations revealed the new satellite (Showalter, 1991).

Saturn will be studied by the Cassini orbiter and the Huygens Titan Probe. It is hoped that Saturn's gravity field will be determined to a 2nd degree and order with possible higher zonal harmonics. As Cassini loops through the Saturnian system, encounters with several of the other large moons will fill in information on their masses and mean densities and better characterize the interdynamics of the planet and its satellites (Kliore et al., 1992).

The best information on Uranus comes from the Voyager 2 flyby of the planet between late 1985

30

and early 1986. The combination of Doppler information and visual identification of mutual perturbations between the satellites allowed greatly improved mass determinations for the five major satellites, and therefore produced mean densities and indications of the moons' composition. The compositional information, in fact, led to the conclusion that the satellites could not be captured comets, as had been suggested (see Anderson et al., 1987a, for discussion). Uranus itself gained a more accurate value for both its own mass and the solar-to-Uranian-system-mass ratio, though significant information for other gravitational field parameters was not obtained. A model of Uranus' gravity field would be particularly interesting as Uranus is the only planet whose axis of rotation appears nearly parallel to the ecliptic plane.

Neptune was the last encounter for Voyager 2, in mid 1989. Because of the close approach and the past difficulties in obtaining information about such a distant planet using only earthbound techniques, the Voyager flyby was able to increase the accuracy of the solar-to-Neptunian-system-mass ratio by a factor of 1000, using both navigation and Doppler data (Tyler et al., 1989). From the data, the masses of Neptune and Triton were estimated to 0.0003% and 0.3%, respectively. Even the small satellites Nereid and 1989N1 were observable in the spacecraft Doppler signature (Tyler et al., 1989). Estimates of a few, low order coefficients of the Neptunian gravity field were also obtained. A discussion of the interior structure of Neptune appears in Hubbard et al., 1991.

Pluto has yet to be approached by spacecraft, although there are studies for a possible future mission. As with Neptune, the increase in volume and accuracy of information from a spacecraft encounter over current Earth-based observations would be enormous.

Most asteroids are too small to produce noticeable effects on spacecraft. Galileo's 1991 encounter with the asteroid Gaspra produced only images. In 1993, however, Galileo is scheduled to fly by the asteroid Ida, and it is expected that the relatively close approach to Ida will yield the first experimentally measured estimate of an asteroid's mass and therefore density. The corresponding constraints on its composition will allow new insight into theories of the evolution of the solar system and asteroid belt.

It is interesting to note that over an 18-year period (1962-1980), the basic ground system Network-generated Doppler accuracy has improved 50 fold, from 5 mm/sec in 1962 to 0.1 mm/sec in 1980. In 1992, Mars Observer is predicting a 0.01 mm/sec accuracy in overall ground system performance.
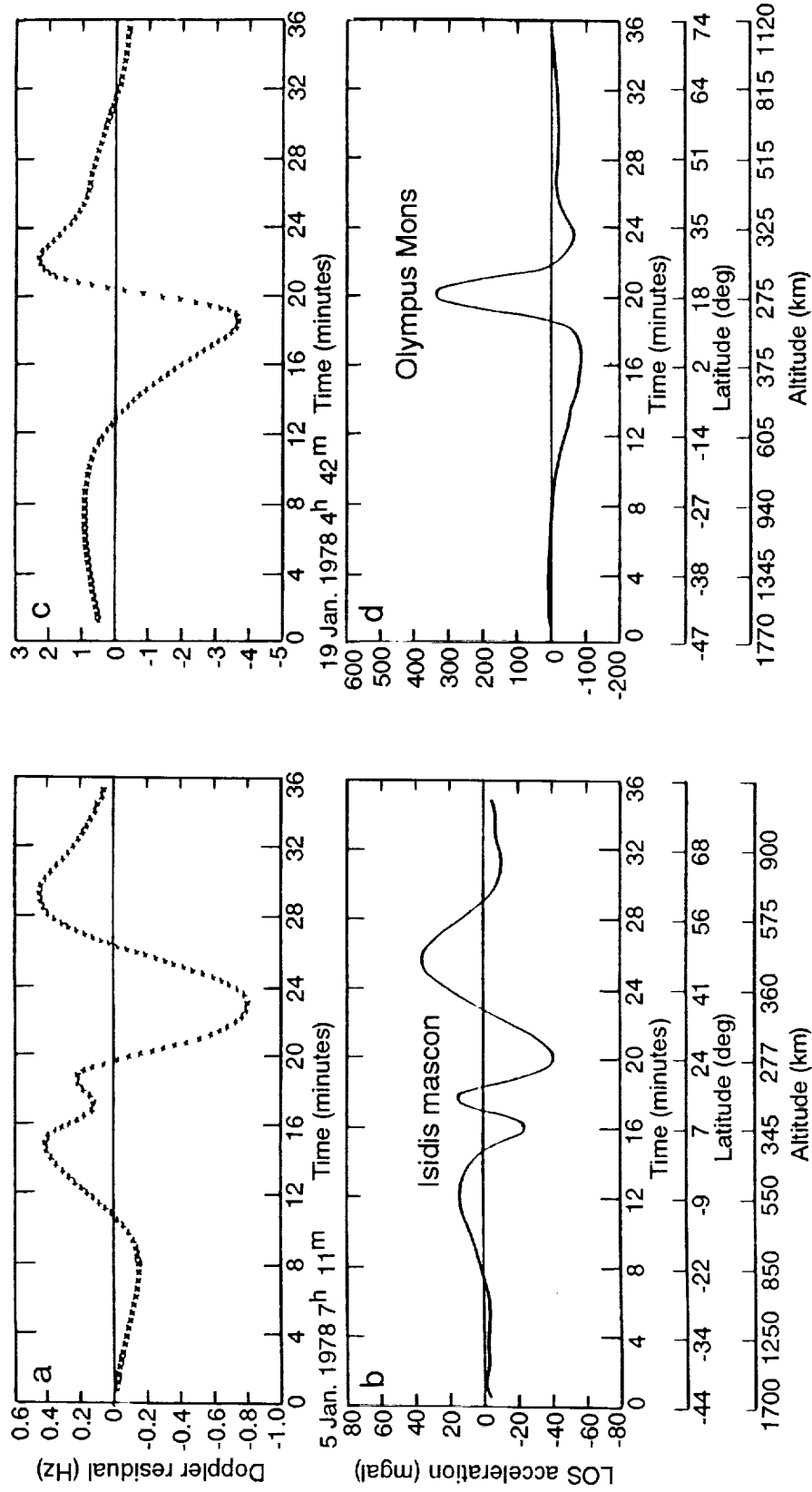
Figure 10. Doppler residuals and line-of-sight acceleration: (a) and (b) over Isidis Planitia, (c) and (d) over Olympus Mons; 1 Hz = 65 mm/second (from Sjogren 1979)
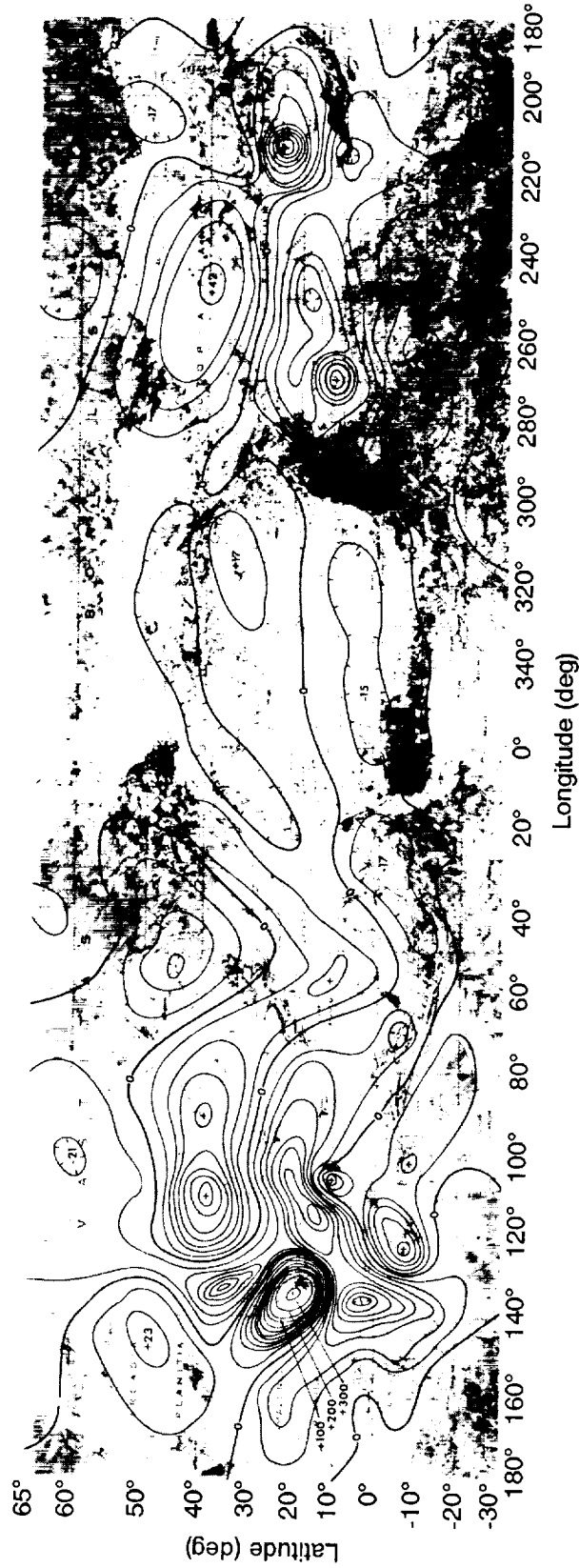
Figure 11. Contoured line-of-sight accelerations. Contours are at 10-mgal intervals, except those notated at Olympus Mons (18° N, 133° W). These accelerations are in addition to a 4th-degree and order background field. Accelerations are at spacecraft altitudes that were approximately 1000 km at 70° N, 300 km at 25° N, and 1000 km at 30° S (from Sjogren, 1979)

VI. Search for Low-Frequency Gravitational Radiation

Gravity is described theoretically as a curvature of space-time. When a massive physical system undergoes violent dynamics, the curvature varies with time, radiating waves of space-time curvature (gravitational waves). Detection and subsequent detailed study of gravitational waves have the potential to revolutionize our view of the Universe. As emphasized by Thorne (1987, 1991), gravitational waves offer a "new window" for observational astronomy, giving information fundamentally different from that available in the electromagnetic window. The experimental difficulty with direct detection is that gravitational waves interact so weakly with matter. This extremely weak interaction will be an advantage in ultimate detections since the waves received will have propagated essentially unchanged from their sources; information about the time evolution of sources during violent events will have been preserved, unconfused by subsequent absorption or scattering. Relativistic motion of bulk matter and strong gravitational fields are central to theoretical views about violent activity in, for example, galactic nuclei and quasars. Gravitational waves from these objects will give us the first observations of the interiors of these strong-gravity, high-velocity regions.

A gravitational wave is a propagating, polarized gravitational field--a "ripple" in the curvature of space-time. These waves are predicted by all relativistic theories of gravity. However, different theories of gravity predict different properties of the radiation (e.g., propagation speed, generation mechanism, and polarization properties). The waves are characterized by their effects on separated test masses and separated clocks. The waves are propagating strain of spacetime, hence their amplitudes are dimensionless strain amplitudes (gravitational potential/c^2) that change the fractional difference in distance between test masses and the rates at which separated clocks keep time.

In Einstein's theory of general relativity, gravitational waves are propagating solutions of the Einstein field equations. These waves carry energy and momentum. As with electromagnetic waves, gravitational waves are transverse to the propagation direction, have two independent polarizations, and propagate at the speed of light. However, unlike electromagnetic waves, gravitational waves couple to all matter (not just charged matter) and are extremely weak: the ratio of gravitational forces to electrical forces is about 10^{-40}. This extreme weakness has two

consequences: (1) gravitational waves are generated at detectable levels only by very massive sources under violent dynamical conditions (that is, astrophysical sources), and (2) the waves thus produced propagate unchanged from their sources, unaffected by scattering or absorption due to intervening matter. As mentioned above, this means that detections give information on the interiors of high gravity, high velocity regions not obtainable by other means.

Alternate relativistic theories of gravity also agree on the existence of gravitational waves. Those theories differ, however, in essential features of the radiation: the number of polarization states, propagation speed, and efficiency of wave generation.

Observationally, the strength of a gravitational wave is characterized by the fractional distance change between two test masses that is induced by the wave: the dimensionless "strain amplitude," $h = \Delta \ell / \ell_0$, where ℓ_0 is the unperturbed distance between the masses.

Gravitational waves are conventionally classified on the basis of their temporal behavior: *bursts* are "on" for a well-defined time that is short compared to the observing interval, *periodic waves* have power concentrated at a few Fourier harmonics (having amplitude and phase that are sensibly constant over the observing interval), and *stochastic waves* have random variation over a time that is long compared with the observing interval. Hybrid waveforms can also exist, e.g., quasi-periodic chirp waves.

Bursts (which last for at most a few cycles) could be produced on a variety of time scales by collisions of stars or black holes, supernovae collapse to a neutron star, collapse of a star or star cluster to form a black hole, final coalescence of compact binaries (neutron stars and black holes), and the fall of stars or small black holes into supermassive black holes.

Periodic waves (superpositions of one or more sinusoids that are approximately constant in amplitude and frequency over a typical observing time) could be produced by nonaxisymmetric rotating neutron stars, binary stars, and binary black holes.

Stochastic waves (random fluctuations that persist for times long with respect to the observing interval) will be produced by an ensemble of incoherently radiating binary stars, deaths of pre-galactic massive stars, vibrations of cosmic strings, or, finally, as a relic of inhomogeneity in the structure of the big bang itself.

These waves are produced on a variety of time scales, depending on the masses of the objects involved. In general, stronger gravitational waves are expected to be produced on longer time scales. The time scales and strengths of the gravitational radiation from these sources can be estimated, based on theory and what is known about the universe from electromagnetic observations. Figure 12, adapted in highly simplified form from Thorne (1987), shows the estimated strength and time scale of the radiation for some of these sources. It should be understood that these estimates are highly uncertain; the strength of the source's waves for a given distance from the Earth and the rate of occurrence of that type of source (thus the distance to the nearest one) are often extremely uncertain. This diagram should thus be viewed as current theoretical thinking, with the understanding that actual gravitational wave detections may provide surprises. See Thorne (1987) for a thorough discussion.

Figure 12 shows the upper limit to the anticipated strength of burst sources based on current theoretical understanding. This limit is based on general physical considerations, including the assumptions that we do not live in a special time or place in the universe, that there are no enormous primordial bursts, that no single radiating object in the galaxy has a mass greater than 100 million solar masses, and that there is no significant beaming of the radiation from the strongest sources.

The "closure density" shown in figure 12 is the envelope of the family of curves having a bandwidth equal to a center frequency that represents the level of a stochastic gravitational wave background having energy-density sufficient to gravitationally close the universe. "Collapse to black hole" is the anticipated strength for burst radiation from black hole formation, assuming the mass of the hole (indicated) and assuming the source is at the Hubble distance (3 Gpc) or the Virgo cluster (where the amplitudes would be about 200 times larger). The shaded area labeled "black hole binaries (Hubble distance)" indicates the amplitudes of periodic radiation from black hole binaries of indicated mass at the Hubble distance. The nearly horizontal arrows indicate evolutionary tracks of these coalescences at the Hubble distance. These would produce periodic and chirp radiation culminating in bursts at the time of coalescence. Amplitudes again scale upwards by about 200 for sources in the Virgo cluster. "Known galactic binary stars" shows the calculated strength of periodic waves from known binary stars in our galaxy. "Compact binaries" shows the calculated amplitudes for compact binaries, e.g., neutron star binaries, in our galaxy. Loosely, this diagram resolves into three spectral bands: high frequencies (>10 Hz), low

frequencies ($\sim 10^{-4}$ to 10^{-1} Hz), and ultra-low frequencies ($< 10^{-7}$ Hz). Detection approaches are different in each band.

Noise (notably seismic noise) causes ground-based detectors to be most sensitive to short-duration waves. There are two ground-based methods: resonant bars and laser interferometers (Michelson et al., 1987; Abramovici et al., 1992). Bar technology was pioneered in the 1960s by J. Weber of the University of Maryland. In a resonant bar antenna, gravitational waves excite mechanical oscillations in the bar; these oscillations are read out by a transducer/amplifier system. Current generation cryogenically cooled massive bars now achieve sensitivities of $\sim 10^{-18}$. In laser interferometer antennas, the detector typically consists of three suspended masses arranged at the corners of a right-angle "L." Mirrors are attached to the masses on the ends of the arms and to a beam splitter on the corner mass. A gravitational wave incident on the system pushes the masses in one arm together while pushing the masses on the other arm apart. This is reversed on the next half cycle of the wave. The relative motions caused by the wave are detected as a fringe shift in a laser interferometer system monitoring the masses. The system is inherently broadband; many Fourier components are measured and thus the gravitational waveform can be constructed. The current generation of ground-based beam detectors has sensitivity comparable to that of resonant bars for $\sim$kHz frequency waves. The Caltech/MIT LIGO (Laser Interferometer Gravitational-Wave Observatory) collaboration is moving forward with construction of a pair of very large beam detectors (4 km arms) with more than three orders of magnitude better sensitivity expected.

Isolation of the test masses from seismic noise, other acoustic noise from the environment, and fluctuating gravity gradients is prohibitively difficult. Therefore, for observations in the "low-frequency" (less than about 10 Hz), spectral band, the detectors must be space based.

Space-based detectors are sensitive at low frequencies because of the large characteristic scale of the experiments (mass separations are approximately in astronomical units) and because of the low "environmental noise" in space. The current generation of space-based detectors uses the Earth and a distant spacecraft as free test masses. The Doppler tracking system of the Deep Space Network, driven by an ultra-high-quality frequency standard on the ground, monitors a transponded microwave link with a distant spacecraft. In doing so, it continuously measures the relative dimensionless velocity ($\Delta v/c$) between the Earth and spacecraft. A gravitational wave passing through the solar system produces a strain of $\Delta \ell / \ell_0$ on the Earth-spacecraft system and

proportionately shifts the frequency of the clock driving the Doppler system. The result (figure 13) is that the gravitational waveform is replicated three times in the Doppler tracking time series: once when the wave "buffets" the Earth, causing a small change in the difference between the transmitted and received Doppler frequencies; once when the spacecraft is buffeted by the wave, causing the signal transponded at an intermediate time to be different than the transmitted signal; and once when the initial Earth perturbation is transponded back to the Earth at a "two-way light-time" after the initial pulse. This three-pulse response is an important signature of a gravitational wave and allows discrimination against noise sources in the Doppler measurement system that have different response functions.

The amplitudes of the three pulses are such that the areas of the three pulses add to zero. This defines the low frequency band edge in spacecraft observations: as the pulse duration becomes comparable to the two-way light-time between the Earth and the spacecraft, the pulses begin to overlap and cancel to first order. The high-frequency band edge is ~0.1 Hz, set by a combination of thermal noise in the receiver and frequency standard and (for some spacecraft) high-frequency unmodeled motion of the spacecraft.

At ultralow frequencies, pulsar timing can be used to search for stochastic waves from the early universe. The idea is that the rotation of the pulsar is a highly accurate "clock." If a gravitational wave is incident on the pulsar (or Earth), the rate at which the pulsar "clock" (or Earth clocks) keeps time is changed. Thus pulsar timing residuals can be used to constrain the spectral density of random gravitational wave perturbations at ultralow frequencies. For a review, see Section 5 of Thorne (1987), and references therein.

The technique of relevance to the Deep Space Network is the Doppler technique. In this section, some of the details of this technique are given, and a discussion of the ultimate sensitivity of the technique is given. As outlined previously, the Doppler tracking measures the relative dimensionless velocity $\Delta v/c = \Delta f/f_0$ of Earth and spacecraft as a function of time, where Δf is the perturbation in the Doppler frequency and f_0 is the nominal radio frequency of the link. A gravitational wave of strain amplitude h incident on the system causes small perturbations in the tracking record. These perturbations are of order h in $\Delta f/f_0$ and are replicated three times in the Doppler data (Estabrook and Wahlquist 1975). That is, the "signal part" of the observed Doppler time series is the convolution of the waveform

39

$$g(t) = (1 - \mu^2)^{-1}\{\mathbf{n} \cdot [h_+(t)\, e_+ + h_x(t)\, e_x] \cdot \mathbf{n}\}$$

with the function

$$[(\mu - 1)/2]\, \delta(t) - \mu\, \delta[t - (1 + \mu)L/c] + [(1 + \mu)/2]\, \delta(t - 2L/c)$$

where μ is the cosine of the angle between the Earth-spacecraft vector and the gravity wave vector and L is the Earth-spacecraft distance, $\mathbf{n}$ is a unit vector from the Earth to the spacecraft, and e_+, e_x are transverse, traceless polarization tensors (Estabrook and Wahlquist 1975; Wahlquist 1987). The sum of the Doppler perturbations of the three pulses is zero; pulses having duration longer than about the one-way light-time produce overlapping responses in the tracking record, and the observed response then cancels to first order. The tracking system thus has a natural passband to gravitational excitation: the low-frequency band edge is set by pulse cancellation to be approximately 1/one-way light-time, while thermal noise in the radio system and short term stability of the frequency standard limits the high-frequency response to an order of 0.1 Hz.

Gravitational waves must be detected in the presence of noise. Experience to date indicates that the Doppler time series is adequately modeled as

$$y(t) = \Delta f/f_0 = \text{gravity waves + propagation noise + clock noise + thermal noise + systematic errors}$$
$$= \{[(\mu-1)/2]\delta(t) - \mu\delta[t-(1+\mu)L/c] + [(1+\mu)/2]\delta(t-2L/c)\} * g(t)$$
$$+ \{\delta(t) + \delta[t-2(L)/c]\} * \text{troposphere}(t)$$
$$+ \{\delta(t) + \delta[t-2(L-x)/c]\} * \text{plasma}(t)$$
$$+ \{\delta(t) - \delta(t-2L/c)\} * \text{clock}(t)$$
$$+ \text{thermal}(t)$$
$$+ \text{systematic errors}$$

where $*$ indicates convolution, $g(t)$ is the scalar gravitational waveform (produced by the tensor wave's interaction with the Earth-spacecraft system), and "troposphere," "plasma," "clock" and "thermal" are noise processes, L is the distance to the spacecraft, and x is the distance to the equivalent solar wind "phase screen" ($x \approx 0.25$ AU for experiments done near solar opposition). Slowly varying systematic errors are, at current and near-future sensitivity levels, significant mainly for burst wave searches when the radio tracking beam is at low elevation angles.

Note that the plasma and clock noises enter in essentially orthogonal ways and are different from

the three-pulse response. This was noted by Estabrook and Wahlquist (1975) and can be exploited to improve signal-to-noise ratio (sometimes dramatically) over what one might expect. (For a discussion of noise sources and their transfer functions to the Doppler observable, see Wahlquist et al., 1977, or Armstrong, 1989).

Searches for gravitational waves in the low-frequency band have used the Viking, Voyager, and Pioneer spacecraft to determine upper limits for gravitational wave strengths (Anderson, 1977; Armstrong et al., 1979; Hellings et al., 1981; Anderson et al., 1984; Anderson and Mashhoon, 1985; Armstrong et al., 1987; Estabrook, 1988; Anderson et al., 1990). All such searches have been limited at low frequencies by plasma propagation noise. The best sensitivities to date are for periodic waves: 7×10^{-15} (one sigma) (Anderson et al., 1992b).

Near-future observations will use the Galileo, Ulysses, and Mars Observer spacecraft (Estabrook, 1988; Bertotti et al., 1992). Especially noteworthy is a coincidence experiment involving Mars Observer, Galileo, and Ulysses in the Spring of 1993. Expected sensitivity for periodic waves in that experiment is $\sim 10^{-15}$ (set by the X-band plasma scintillation noise on Mars Observer).

In the late 1990s the Cassini spacecraft, with a Ka-band radio link and ultrastable ground and spacecraft electronics, will be used for much higher sensitivity observations. An engineering study (Riley et al., 1990) indicates that sensitivity to periodic waves could be $\sim 10^{-16}$ for one month of tracking near solar opposition, set by the ability to monitor and remove phase scintillations due to the wet troposphere.

Sensitivity improvements in the low-frequency band significantly better than those possible with Ka-band and precision tropospheric monitoring will probably require moving both the test masses into space. This would remove the problem of tropospheric correction and the host of unmodeled geophysical effects (e.g., microseismic activity and unmodeled Earth tide effects) that become important at these very sensitive levels. One possibility, promising but not yet studied in detail, is to use a distant spacecraft coupled with a deep space station in a suitable Earth orbit as the two test masses.
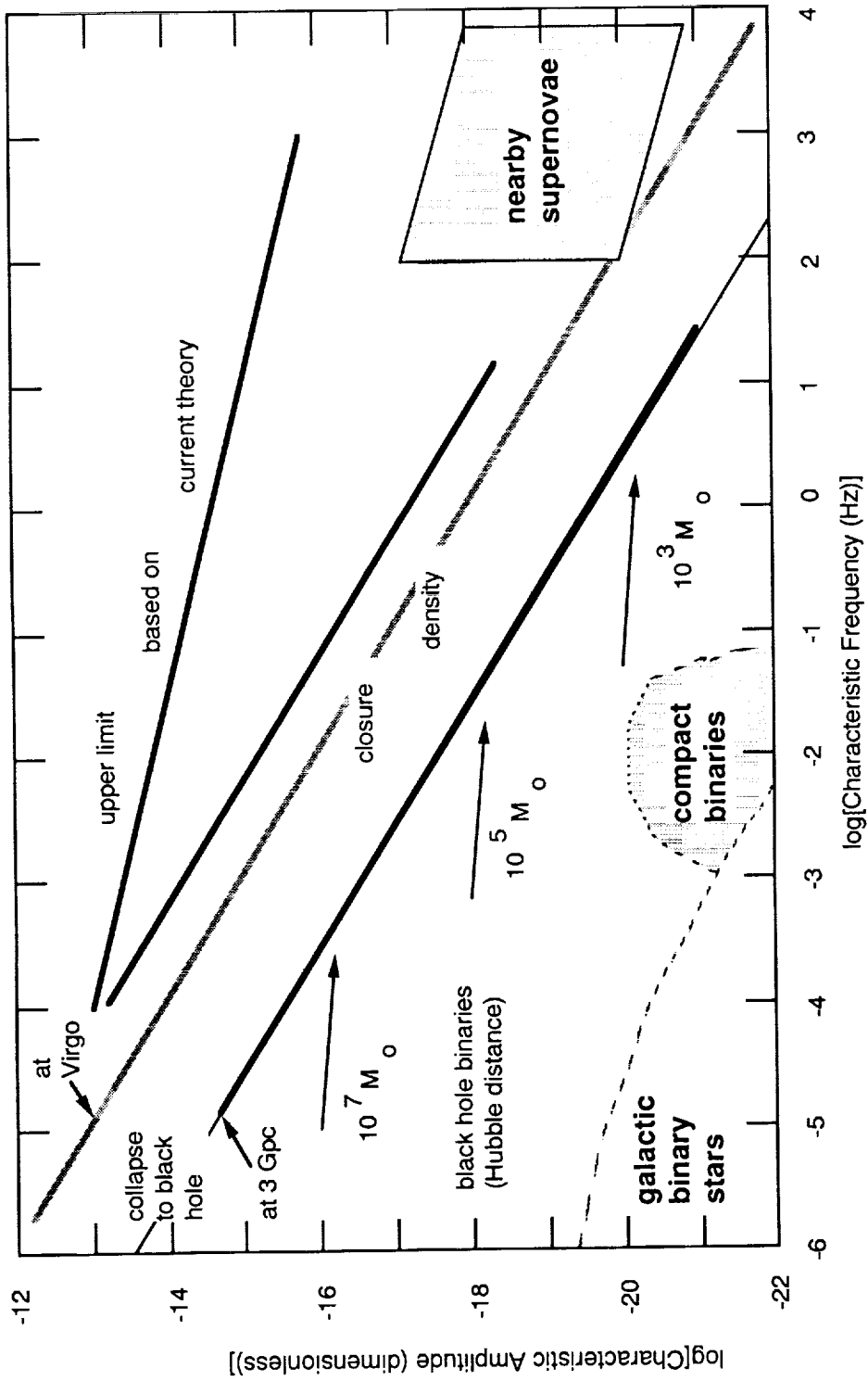
Figure 12. Estimated strengths and gravitational wave radiation sources

Spacecraft

L

θ

Earth

Z

Gravitational
Wave

Z

Earth buffeting

$\dfrac{\Delta \nu}{\nu}$

Spacecraft
buffeting

$(1 + \cos \theta)$ L/c

2 L/c

Earth buffeting,
transponded
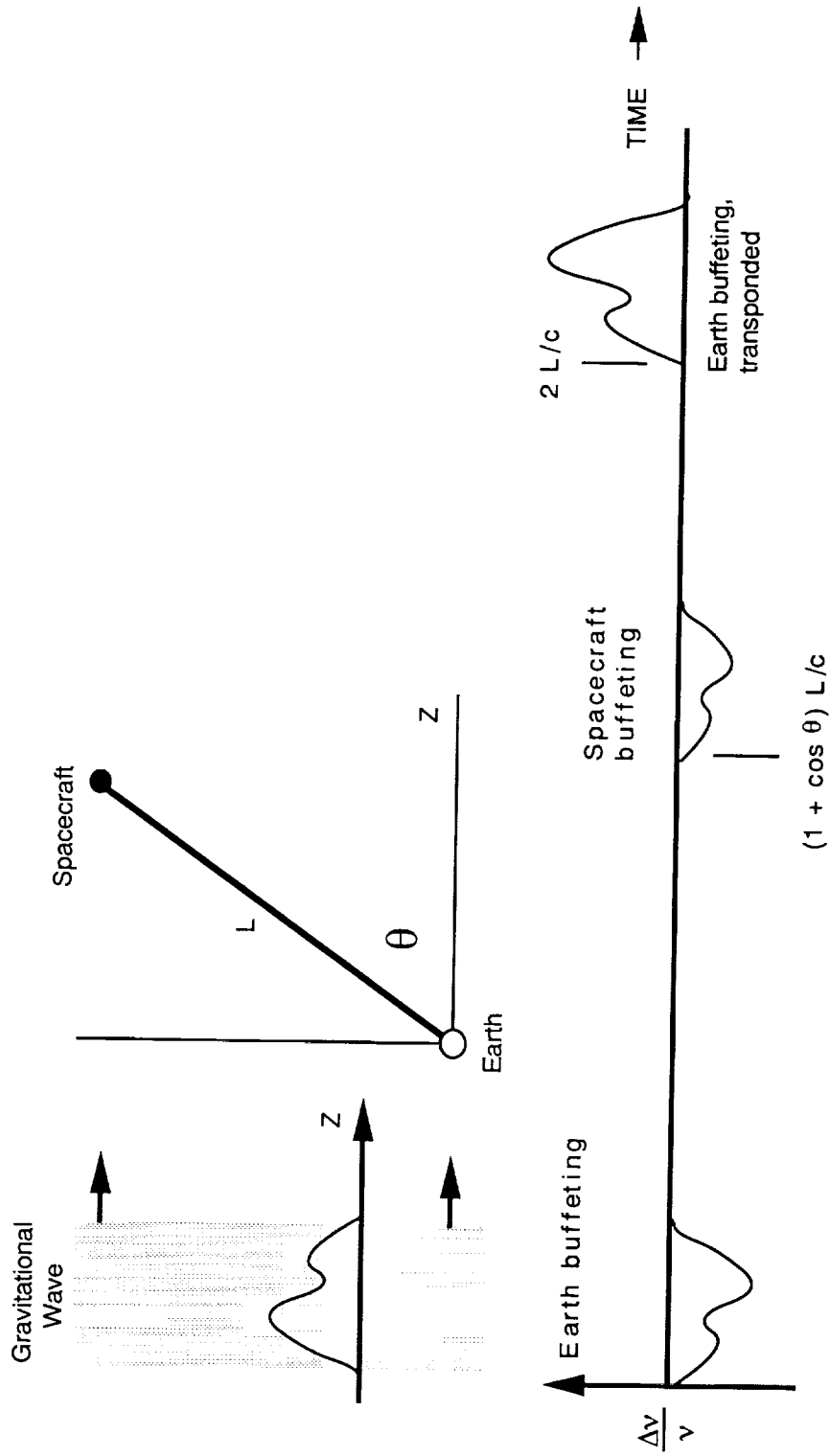
TIME

Figure 13. Gravitational wave form three-pulse response in Doppler measurements

43

VII. Measurements of Relativistic Time-Delay

One of the most exciting aspects of the capability to obtain range measurements from spacecraft in solar conjunction phases is a test of a portion of Einstein's theory of general relativity that predicts that electromagnetic waves passing close to massive bodies (e.g., the Sun) are delayed by the gravitational field. The signal time delay is dependent upon the observer-Sun-spacecraft geometry as follows:

$$\Delta t = 2GM_o c^{-3}(1+\gamma) \ln((r_e + r_m + R)(r_e + r_m - R)^{-1})$$

where:

Δt = signal delay, sec

G = gravitational constant, $km^3/kg/sec^2$

M_o = solar mass, kg

c = speed of light, km/sec

r_e = Earth-Sun distance, km

r_m = Sun-spacecraft distance, km

R = Earth-spacecraft distance, km

In Einstein's theory of general relativity, the (parameterized post-Newtonian) parameter γ is replaced by 1. Hence the nature of the experiment is to verify that γ indeed equals 1.

To measure signal time delay, the Deep Space Network uses a binary coded sequential-acquisition ranging system. The hardware is called the Sequential Ranging Assembly (the predecessor to that was the Planetary Ranging Assembly). Ranging data are described in Section II.

The first major attempt to measure the relativistic time-delay of a spacecraft signal occurred during the solar conjunction of Mariners 6 and 7 during mid-1970 (Anderson et al., 1975). This experiment was able to verify the value of γ to about 6%, i.e., $\gamma = 1.00 \pm 0.06$. The major error source that prevented that experiment from achieving greater accuracy was the non-gravitational forces on the spacecraft, which limited the accuracy of the orbit determination. Additionally, uncertainties in the signal delay caused by the scattering of free electrons in the solar corona

contributed an error of about 2% to the determination of γ from Mariners 6 and 7. Later, non-gravitational acceleration noise was reduced by the Mariner 9 Mars Orbiter, and a measurement of γ to the 2% level was achieved (Anderson et al., 1978; Reasenberg and Shapiro, 1977).

During 1976-1977, the relativistic experiment was performed using both the Viking Mars Orbiter and Lander spacecraft (Shapiro et al., 1977; Cain et al., 1978; Reasenberg et al., 1979). Three factors led to a very significant improvement in accuracy over the earlier Mariner experiments:

(1) Significant improvement was made in the ground equipment; in particular the ability to calibrate the ground system ranging delay.

(2) The availability of a landed spacecraft. The highly precise knowledge of the landed spacecraft's location eliminated the much larger positional errors of heliocentric spacecraft, such as those due to orbital errors and unmodeled forces.

(3) Dual-frequency downlink (S- and X-band) capability. The dual-frequency downlink of the orbital spacecraft permitted accurate measurements of the signal delay due to electron density, thus significantly reducing the plasma uncertainty, which had previously been the largest error source.

Independent determination of the parameter γ at the Jet Propulsion Laboratory and Massachusetts Institute of Technology led to a value of 1 ± 0.002, the most accurate test of the radar time-delay to date (see Anderson et al., 1986, for a more detailed review).

Since the Viking experiment, a test of the solar relativistic time-delay was performed with the Voyager 2 spacecraft during solar conjunction in December of 1985, shortly before the Uranus encounter in January of 1986 (Krisher et al., 1991b). The ranging system was similar to that used for Viking, with an S-band uplink and dual S- and X-band downlinks. For Viking, dual-band ranging was possible only with the orbiters, not the landers. Therefore, calibration of plasma delay to the landers could be done only indirectly by using the orbiter ranging data. With Voyager, it was possible for the first time to calibrate directly the plasma delay on the downlink. In addition, the conjunction was close to the solar equator, which minimized latitudinal variations in the solar plasma density (Anderson et al., 1987b). A remaining limitation in the Voyager experiment was non-gravitational accelerations of the spacecraft due to attitude control activity. This was

modeled by using telemetry records of thruster pulse firing. The final result was a determination of $\gamma = 1 \pm 0.03$.

Another relativistic time-delay test was attempted during the solar conjunction of Voyager 2 in 1988. Because of the increased range to the spacecraft, three-way ranging was necessary for many passes. This provided an opportunity to calibrate accurately the plasma delay on the single frequency uplink by using the preceding, overlapping dual-band downlink measurements. Unfortunately, three-way ranging was still under development in the Network and much of the ranging data were corrupted by code-synchronization errors. These errors could be canceled by differencing the dual-band range measurements, thereby providing useful measurements of coronal electron density during solar maximum activity in the 11-year cycle (Krisher et al., 1991a). It was not possible, however, to obtain an interesting test of the relativistic time-delay.

VIII. Spacecraft Deceleration in Cometary Comae

The Giotto spacecraft encountered comet P/Halley on 13 March 1986 (Edenhofer et al., 1987) and comet P/Grigg-Skjellerup on 10 July 1992 (Pätzold et al., 1993). The scientific objective of the Giotto radio science experiment was the determination of the cometary mass flux (gas and dust) on the spacecraft by observing its change in velocity during the flight through the cometary atmosphere (coma). In principle, the change in velocity due to cometary dust drag can be determined using three different radio navigational techniques. Two of these, based on two-way ranging and Doppler observations (S-band uplink, S- or X-band downlink), were conducted after the last pre-encounter spacecraft maneuver (two days before closest approach to the nucleus) and before the first post-encounter maneuver (one day after closest approach). During the actual encounter period, the X-band one-way downlink frequency (third technique) was recorded in real time.

Comparison of the pre- and post-encounter two-way coherent Doppler and ranging residuals yields the total change in the spacecraft's radial velocity at encounter. These data were recorded at rates of one Doppler sample per second and one ranging point per ten minutes. Knowing the flyby geometry, one can compute the total change in spacecraft velocity along the relative flyby velocity vector and, from this result, the total impacted effective mass. Table 2 summarizes the results from the Halley and Grigg-Skjellerup flybys.

The change in velocity as a function of time can also be extracted from the one-way noncoherent downlink frequency recorded during the actual encounter (closed-loop: 10 samples per second; open-loop: 50,000 samples per second). During the Halley flyby, it was obvious that the deceleration was not continuous, occurring rather in distinct steps interpreted as separate traversals of successive dust jets emanating from the nucleus surface. Unfortunately, a similar observation was not possible during the Grigg-Skjellerup flyby because the deceleration was below the noise level. Electrical and/or mechanical disruptions of the radio system were incurred. These were presumably caused by dust particle impacts on the spacecraft that generated frequency disturbances superimposed on the true Doppler frequency shift. Much larger Doppler shifts were observed in the one-way data than in the two-way data (16.9 Hz instead of 4.6 Hz at Halley; 124 Hz instead of 11 mHz at Grigg-Skjellerup).

Other changes in Giotto's dynamical state (nutation and spin rate) could be detected in addition to the deceleration (see Table 2). These were caused by impacts of very large dust particles (larger than 10 mg). The mass of the largest particle at Halley (about 400 mg) was estimated from a statistical analysis. At Grigg-Skjellerup, the nutation and spin rate changes could be most plausibly explained by one single dust particle of at least 30 mg out of the total impacted mass of 39 mg.

Table 2. Comparison between Giotto flyby parameters at Comets Halley and Grigg-Skjellerup (GS)

Parameter	Halley	GS
Relative flyby velocity, km/sec	68.37	13.99
Angle between relative velocity and spacecraft spin axis, deg	0	68.8
Angle between relative flyby velocity and direction to Earth, deg	44.2	67.3
Distance to Earth, AU	0.9	1.4
Distance of closest approach, km	596	<200
Spacecraft mass, kg	574	529
Change in radial velocity, mm/sec	−167	−0.4
Total change in velocity, mm/sec	−230.5	−1.0
Impacted effective mass, mg	1932	39
Change in spin period, msec	+12	−1
Nutation angle, deg	1.04	0.10
Largest impacted particle, mg	≈400	≈30

References and Bibliography

Abramovici, A., W. E. Althouse, R. W. P. Drever, Y. Gursel, S. Kawamura, F. J. Raab, D. Shoemaker, L. Sievers, R. E. Spere, K. S. Thorne, R. E. Vogt, R. Weiss, S. E. Whitcomb, M. E. Zucker, "LIGO: The Laser Interferometer Gravitational-Wave Observatory," *Science*, Vol. 256, p. 325, 1992.

Anderson, J. D., and M. R. Warner, "Determination of the Masses of the Moon and Venus, and the Astronomical Unit from Radio Tracking of Mariner II," in *Trajectories of Artificial Celestial Bodies*, pp. 216-246, Springer-Verlag, New York, 1966.

Anderson, J. D., "Geodetic and Dynamical Properties of Planets," *EOS*, Vol. 5, pp. 515-523, 1974.

Anderson, J. D., P. B. Esposito, W. Martin, C. L. Thornton, and D. O. Muhelman, "Experimental Test of General Relativity Using Time-Delay Data From Mariner 6 and Mariner 7," *Astrophysical Journal*, Vol. 200, pp. 221-233, 1975.

Anderson, A. J., "Detection of Gravitational Waves by Spacecraft Doppler Data," *Atti dei Convengi Lincei*, Vol. 34, p. 235, 1977.

Anderson, J. D., M. S. W. Keesey, E. L. Lau, E. M. Standish, Jr. and X X Newhall, "Tests of General Relativity Using Astrometric and Radio Metric Observations of the Planets," *Astronautica*, Vol. 5, pp. 43-61, 1978.

Anderson, J. D., G. W. Null, E. D. Biller, S. K. Wong, W. B. Hubbard, and J. J. MacFarlane, "Pioneer Saturn Celestial Mechanics Experiment," *Science*, Vol. 207, pp. 449-453, 1980.

Anderson, J. D., J. W. Armstrong, F. B. Estabrook, R. W. Hellings, E. K. Lau, and H. D. Wahlquist, "Pioneer 10 Search for Gravitational Waves - No Evidence for Coherent Radiation from Geminga," *Nature*, Vol. 308, p. 158, 1984.

Anderson, J. D., and B. Mashhoon, "Pioneer 10 Search for Gravitational Waves - Limits on a Possible Cosmic Background in the Microhertz Region," *Astrophysical Journal*, pp. 290, 445, 1985.

Anderson, J. D., G. Colombo, P. B. Esposito, E. L. Lau, and G. B. Trager, "The Mass, Gravity Field, and Ephemeris of Mercury," *Icarus*, Vol. 71, pp. 337-349, 1986a.

PRECEDING PAGE BLANK NOT FILMED

Anderson, J. D., G. S. Levy, and N. A. Renzetti, "Application of the Deep Space Network (DSN) to the Testing of General Relativity, in Relativity" in *Celestial Mechanics and Astrometry*, IAU Symposium No. 114, Kovalevsky and Brumberg (eds.) pp. 329-344, D. Reidel, Dordrecht, Holland, 1986b.

Anderson, J. D., J. K. Campbell, R. A. Jacobson, D. N. Sweetnam, A. H. Taylor, A. J. R. Prentice, and G. L. Tyler , "Radio Science with Voyager 2 at Uranus: Results on Masses and Densities of the Planet and Five Principal Satellites," *Journal of Geophysical Research*, Vol. 92, pp. 14877-14883, 1987a.

Anderson, J. D., T. P. Krisher, S. E. Borutzki, M. J. Connally, P. M. Eshe, D. L. Gresh, H. B. Hotz, S. Kinslow, E. R. Kursinski, L. B. Light, S. M. Matousek, K. I. Moyd, P. A. Rosen, D. C. Roth, D. N. Sweetnam, A. H. Taylor, and G. L. Tyler, "Radio Range Measurements of Coronal Electron Densities at 13 and 3.6 Centimeter Wavelengths During the 1985 Solar Conjunction of Voyager 2," *Astrophysical Journal* Vol. 323, pp. L141-L143, 1987b.

Anderson, J. D., J. W. Armstrong, and E. L. Lau, "Applications of Hydrogen Maser Technology to the Search for Gravitational Radiation," in Proceedings of the 21st Annual Precise Time and Time Interval (PTTI) Applications and Planning Meeting, U. S. Naval Observatory, Time Service Department, Washington, D. C., 1990.

Anderson, J. D., S. W. Asmar, J. K. Campbell, R. A. Jacobson, T. P. Krisher, E. R. Kursinski, E. L. Lau, and D. D. Morabito, "Gravitational Parameters for Neptune and Triton," Neptune and Triton Conference, Tucson, AZ, 6-10 January, 1992a.

Anderson, J. D., J. W. Armstrong, E. L. Lau, "Upper Limits for Gravitational Radiation from Supermassive Coalescing Binaries," accepted by *Astrophysical Journal*, 1992b.

Anderson, J. D., J. W. Armstrong, J. K. Campbell, F. B. Estabrook, T. P. Krisher, and E. L. Lau, "Gravitation and Celestial Mechanics Investigations with Galileo," *Space Science Reviews*, Vol. 60, pp. 591-610, 1992c.

Armstrong, J. W., R. Woo, and F. B. Estabrook, "Interplanetary Phase Scintillations and the Search for Very Low Frequency Gravitational Radiation," *Astrophysical Journal*, Vol. 30, pp. 574, 1979.

Armstrong, J. W., F. B. Estabrook, and H. D. Wahlquist, "A Search for Sinusoidal Gravitational Radiation in the Period Range 30-2000 Seconds," *Astrophysical Journal*, Vol. 318, p. 536, 1987.

Armstrong, J. W., "Spacecraft Gravitational Wave Experiments," in *Gravitational Wave Data Analysis*, ed. B. F. Schutz, North Holland: Kluwer Academic Publishers, 1989.

Armstrong, J. W., R. Woo and C. Chang, "Solar Cycle Dependence of Interplanetary Disturbances Observed as Doppler Scintillation Transients by Pioneer Venus Within 0.3 AU," *EOS*, Vol. 73, p. 237, 1992.

Asmar, S. W., and E. R. Kursinski, "The Role of Clocks in Operating Deep Space Missions," in *Proceedings of Precise Time & Time Interval*, 23rd Annual Meeting, Pasadena, California, 3-5 December 1991.

Asmar, S. W., and R. G. Herrera (eds.), *Radio Science Handbook*, Jet Propulsion Laboratory, Pasadena, California, Internal Document, D-7938, Vol. 4, 1993.

Balmino, G., B. Moynot, and N. Vales, "Gravity Field Model of Mars in Spherical Harmonics up to Degree and Order Eighteen," *Journal of Geophysical Research*, Vol. 87, pp. 9735-9746, 1982.

Berman, A. L., and J. A. Wackley, "Doppler Noise Considered as a Function of the Signal Path Integration of Electron Density," *DSN Progress Report* 42-44, pp. 197-202. Jet Propulsion Laboratory, Pasadena, California, 1976.

Berman, A. L., "Solar Wind Turbulence Models Evaluated via Observations of Doppler RMS Phase Fluctuation and Spectral Broadening in the Inner Corona," *DSN Progress Report*, 42-44, pp. 197-202. Jet Propulsion Laboratory, Pasadena, California, 1978a.

Berman, A. L., "Solar Wind Density Fluctuation and the Experiment to Detect Gravitational Waves in Ultraprecise Doppler Data," *DSN Progress Report* 42-44, pp. 189-196, Jet Propulsion Laboratory, Pasadena, California, 1978b.

Berman, A. L., "A Unified Observational Theory for Solar Wind Columnar Turbulence," *DSN Progress Report* 42-50, pp. 124-131. Jet Propulsion Laboratory, Pasadena, California, 1979a.

Berman, A. L., and R. Ramos, "Pioneer Venus Occultation Radio Science Data Generation," *IEEE Transactions on Geoscience and Remote Sensing GE-18*, pp. 11-14, 1980.

Berman, A. L., J. A. Wackley, and W. H. Hietzke, "A Direct Comparison of Viking 2.3 GHz Signal Phase Fluctuation and Columnar Electron Density Between 2 and 160 Solar Radii," to be submitted to *Journal of Geophysical Research*, 1981.

Bertotti, B., R. Ambrosini, S. W. Asmar, J. P. Brenkle, G. Comoretto, G. Giampieri, L. Iess, A. Messeri, and H. D. Wahlquist, "The Gravitational Wave Experiment," *Astronomy and Astrophysics Supplementary Series*, 92, pp. 431-440, 1992.

Bertotti, B., R. Ambrosini, S. W. Asmar, J. P. Brenkle, G. Comoretto, G. Giampieri, L. Iess, A. Messeri, R. Vecchio, H. D. Wahlquist, *Ulysses Gravitational Wave Experiment Report on the First Opposition*, publication number IFSI-91-25, Istituto di Fisica dello Spazio Interplanetario, Frascati, Italy, December 1991.

Bertotti, B., "The Search for Gravitational Waves with ISPM," in *The International Solar Polar Mission - Its Scientific Investigation*, K. P. Wenzel, R. G. Mardsen and B. Battrick, eds., ESA SP-1050, 1983.

Bird, M. K., H. Volland, C. T. Stelzried, G. S. Levy, and B. L. Seidel, "Faraday Rotation Transients Observed During Solar Occultation of the Helios Spacecraft," in *Study of Traveling Interplanetary Phenomena*, pp. 63-74, D. Reidel, Dordrecht, Holland, 1977.

Bird, M. K., "Coronal Sounding with Occulted Spacecraft Signals," *Space Science Review*, Vol. 33, pp. 99-126, 1982.

Bird, M. K., H. Volland, R. A. Howard, M. J. Koomen, D. J. Michels, N. R. Sheeley, Jr., J. W. Armstrong, B. L. Seidel, C. T. Stelzried, and R. Woo, "White-Light and Radio Sounding Observations of Coronal Transients," *Solar Physics*, Vol. 98, pp. 341-368, 1985.

Bird, M. K., M. Pätzold, H. Volland, P. Edenhofer, H. Buschert, H. Porsche, "Giotto Spacecraft Dynamics During the Encounter With Comet Halley," *ESA Journal*, Vol. 12, pp. 149-169, 1988.

Bird, M. K., and P. Edenhofer, "Remote Sensing Observations of the Solar Corona," in *Physics of the Inner Heliosphere*, R. Schwenn and E. Marsch (eds.), Springer-Verlag, Berlin, pp. 13-97, 1990.

Bird, M. K., "Coronal Structures and Their Relation to the Solar Wind," *Journal of Geomag. Geoelectr.*, Supplement 71-89, 1991.

Bird, M. K., S. W. Asmar, J. P. Brenkle, P. Edenhofer, M. Patzold, H. Volland, "The Coronal Electron Density Distribution Determined from Dual-Frequency Ranging Measurements During the 1991 Solar Conjunction of the Ulysses Spacecraft," Submitted to *Astrophysical Journal*, November 1992a.

Bird, M. K., S. W. Asmar, J. P. Brenkle, P. Edenhofer, M. Pätzold, and H. Volland, "The Coronal-Sounding Experiment," *Astronomy and Astrophysics, Supplementary Series 1*, January 1992b.

Bird, M. K., S. W. Asmar, J. P. Brenkle, P. Edenhofer, O. Funke, M. Patzold, and H. Volland, "Ulysses Radio Occultation Observations of the Io Plasma Torus During the Jupiter Encounter," *Science*, Vol. 257, pp. 1531-1535, September 11, 1992c.

Bird, M. K., H. Volland, M. Pätzold, P. Edenhofer, S. W. Asmar, and J. P. Brenkle, "The Coronal Electron Density Distribution Determined From Dual-Frequency Ranging Measurements During the 1991 Solar Conjunction of the Ulysses Spacecraft," submitted to *Astrophysical Journal*, 1993.

Black, M. T., M. T. Zuber and D. C. McAdoo, "Comparison of Observed and Predicted Gravity Profiles over Aphrodite Terra, Venus," *EOS*, Vol. 69, p. 1295, 1988.

Borderies, N., and C. F. Yoder, "Phobos Gravity Field and its Influence in its Orbit and Physical Librations," *Astronomy and Astrophysics*, Vol. 233, pp. 235-251, 1990.

Borderies, N., P. Goldreich, and S. Tremaine, "Precession of Inclined Rings," *The Astronomical Journal*, Vol. 88, pp. 226-228, 1983.

Borderies, N., P. Goldreich, and S. Tremaine, "The Dynamics of Elliptical Rings," *The Astronomical Journal*, Vol. 88, pp. 1560-1568, 1983.

Borderies, N., P. Goldreich, and S. Tremaine, "Sharp Edges of Planetary Rings," *Nature*, Vol. 299, pp. 209-211, 1982.

Borderies, N., G. Balmino, L. Castel, and B. Moynot, "Study of Mars Dynamics from Lander Tracking Data Analysis," *The Moon and the Planets*, Vol. 22, pp. 191-200, 1980.

Campbell, J. K., and J. D. Anderson, "Gravity Field of the Saturnian System from Pioneer and Voyager Tracking Data," *The Astronomical Journal*, Vol. 97, pp. 1485-1495, 1989.

Campbell, J. K., and S. P. Synnott, "Gravity Field of the Jovian System from Pioneer and Voyager Tracking Data," *The Astronomical Journal*, Vol. 90, pp. 364-372, 1985.

Cain, D. L., J. D. Anderson, M. S. W. Keesey, T. Komarek, P. A. Laing, and E. L. Lau, "Test of General Relativity with Data from Viking Orbiters and Landers," *Bulletin of American Astronomical* Society, Vol. 10, p. 396, 1978.

Cimino, J. B., C. Elachi, A. J. Kliore, D. J. McCleese, and I. R. Patel, "Polar Cloud Structure as Derived from the Pioneer Venus Orbiter," *Journal of Geophysical Research*, Vol. 85, pp. 8082-8088, 1980.

Davies, R. W., "Issues in Gravitational Wave Detection With Space Missions," in *Transactions of the International Conference on Gravitational Waves and Radiations*, pp. 33-45, Centre National de la Recherche Scientifique, Paris, France, 1974.

Deep Space Network, *Flight Project Interface Design Handbook,* Jet Propulsion Laboratory, Pasadena, California, Internal Document, 810-5, Rev. D, July 15, 1988.

Deep Space Network, *Systems Requirements Detailed Interface Design,* Jet Propulsion Laboratory, Pasadena, California, Internal Document 820-13, Rev. A, November 1, 1991.

Dennison, B., G. Melnick, M. Harwit, T. Sato, C. T. Stelzried, and D. Jauncy, "Deflection of Polarised Radiation: Relative Phase Delay Technique," *Nature,* Vol. 273, pp. 33-35, 1978.

Edenhofer, P., M. K. Bird, J. P. Brenkle, H. Buschart, P. B. Esposito, H. Porsche, and H. Volland, "First Results From the Giotto Radio-Science Experiment," *Nature,* Vol. 321, pp. 355-357, 1986.

Edenhofer, P., M. K. Bird, H. Buschert, P. B. Esposito, H. Porsche, and H. Volland, "Measurement Technique of the Giotto Radio-Science Experiment," *Journal of Physics E: Science Instrumentation,* Vol. 20, pp. 768-777, 1987.

Edenhofer, P., M. K. Bird, J. P. Brenkle, H. Buschert, E. R. Kursinski, N. A. Mottinger, H. Porsche, C. T. Stelzried, and H. Volland, "Dust Distribution of Comet Halley's Inner Coma Determined from the Giotto Radio-Science Experiment," *Astronomy and Astrophysics,* Vol. 187, p. 712, 1987.

Eshleman, V. R., G. Fjeldbo, J. D. Anderson, A. Kliore, and R. B. Dyce, "Venus: Lower Atmosphere not Measured," *Science,* Vol. 162, pp. 661-665, 1968.

Eshleman, V. R., G. L. Tyler, J. D. Anderson, G. Fjeldbo, G. S. Wood and T. A. Croft, "Radio Science Investigations with Voyager," *Space Science Reviews,* Vol. 21, pp. 207-232, 1977.

Eshleman, V. R., G. L. Tyler, G. E. Wood, G. F. Lindal, J. D. Anderson, G. S. Levy, and T. A. Croft, "Radio Science with Voyager 1 at Jupiter: Preliminary Profiles of the Atmosphere and Ionosphere," *Science,* Vol. 204, pp. 976-978, 1979a.

Eshleman, V. R., G. L. Tyler, G. E. Wood, G. F. Lindal, J. D. Anderson, G. S. Levy, and T. A. Croft, "Radio Science with Voyager at Jupiter: Initial Voyager 2 Results and a Voyager 1 Measure of the Io Torus," *Science,* Vol. 206, pp. 959-962, 1979b.

Esposito, L. W., N. Borderies, P. Goldreich, J. N. Cuzzi, J. B. Holberg, A. L. Lane, R. B. Pomphrey, R. J. Terrile, J. J. Lissauer, E. A. Marouf and G. L. Tyler, "Eccentric Ringlet in the Maxwell Gap at 1.45 Saturn Radii: Multi-Instrument Voyager Observations," *Science,* Vol. 222, pp. 57-60, 1983.

Esposito, P. B., P. Edenhofer, E. Luneburg, "Solar Corona Electron Density Distribution," *Journal of Geophysical Research,* Vol. 85, pp. 3414-3418, 1980.

Esposito, P. B., J. D. Anderson, and A. T. Y. Ng, "Experimental Determination of Mercury's Mass and Oblateness," in *COSPAR: Space Research, XVII,* edited by M. J. Rycroft and A. C. Stickland, pp. 639-644, Pergamon Press, New York, 1978.

Estabrook, F. B., and H. D. Wahlquist, "Response of Doppler Spacecraft Tracking to Gravitational Radiation," *General Relativity and Gravitation,* Vol. 6, pp. 439-447, 1975.

Estabrook, F. B., "Gravitational Wave Searches with Ground Tracking Antennas," *Acta Astronautica,* Vol. 17, pp. 585-587, 1988.

Fjeldbo, G., "Bistatic Radar Methods for Studying Planetary Ionospheres and Surfaces," SU-64-025, 87 pp., Stanford Electronics Laboratories, Stanford, Calif., 1964.

Fjeldbo, G., and V. R. Eshleman, "The Atmosphere of Mars Analyzed by Integral Inversion of Mariner IV Occultation Data," *Planet Space Science,* Vol. 16, pp. 1035-1059, 1968.

Fjeldbo, G., A. J. Kliore, and V. R. Eshleman, "The Neutral Atmosphere of Venus as Studied with the Mariner V Radio Occultation Experiments," *The Astronomical Journal,* Vol. 76, pp. 123-140, 1971.

Fjeldbo, G., A. Kliore, B. Seidel, D. Sweetnam, and D. Cain, "The Pioneer 10 Radio Occultation Measurements of the Ionosphere of Jupiter," *Astronomy and Astrophysics,* Vol. 39, pp. 91-96, 1975.

Fjeldbo, G., A. Kliore, D. Sweetnam, P. Esposito, B. Seidel, and T. Howard, "The Occultation of Mariner 10 by Mercury," *Icarus,* Vol. 29, pp. 439-444, 1976.

Fjeldbo, G., D. Sweetnam, J. Brenkle, E. Christensen, D. Farless, J. Mehta, B. Seidel, W. Michael, Jr., A. Wallio, and M. Grossi, "Viking Radio Occultation Measurements of the Martian Atmosphere and Topography: Primary Mission Coverage," *Journal of Geophysical Research,* Vol. 82, pp. 4317-4324, 1977.

Goldstein, R. M., *The Superior Conjunction of Mariner IV,* Technical Report 32-1092, Jet Propulsion Laboratory, Pasadena, California, 1967.

Goldstein, R. M., "Superior Conjunction of Pioneer 6," *Science,* Vol. 166, pp. 598-601, 1969.

Gresh, D. L., P. A. Rosen, G. L. Tyler and J. J. Lissauer, "An Analysis of Bending Waves in Saturn's Rings as Seen in Voyager Radio Occultation Data," *Icarus,* Vol. 68, pp. 481-502, 1986.

Hellings, R. W., P. S. Callahan, J. D. Anderson, and A. Moffett, "Spacecraft Doppler Gravity-Wave Detection," *Physical Review D*, Vol. 23, p. 844, 1981.

Hinson, D. P., and G. L. Tyler, "Spatial Irregularities in Jupiter's Upper Ionosphere Observed by Voyager Radio Occultations," *Journal of Geophysical Research*, Vol. 87, pp. 5275-5289, July, 1982.

Hinson, D. P., and G. L. Tyler, "Internal Gravity Waves in Titan's Atmosphere Observed by Voyager Radio Occultation," *Icarus*, Vol. 54, pp. 337-352, 1983.

Hinson, D. P., "Magnetic Field Orientations in Saturn's Upper Ionosphere Inferred from Voyager Radio Occultations," *Journal of Geophysical Research*, Vol. 89, no. A1, pp. 65-73, Jan. 1984.

Hinson, D. P., and J. A. Magalhaes, "Equatorial Waves in the Stratosphere of Uranus," *Icarus*, Vol. 94, pp. 64-91, 1991.

Howard, H. T., G. L. Tyler, P. B. Esposito, J. D. Anderson, R. D. Reasenberg, I. I. Shapiro, G. Fjeldbo, A. J. Kliore, G. S. Levy, D. L. Brunn, R. Dickinson, R. E. Edelson, W. L. Zygielbaum, "Mercury: Results on Mass, Radius, Ionosphere," *Science*, Vol. 185, pp. 179-180, 1974a.

Howard, H. T., G. L. Tyler, G. Fjeldbo, A. J. Kliore, G. S. Levy, D. L. Brunn, R. Dickenson, R. E. Edelson, W. L. Martin, R. B. Postal, B. Seidel, T. T. Sesplaukis, D. L. Shirley, C. T. Stelzried, D. N. Sweetnam, A. I. Zygielbaum, P. B. Esposito, J. D. Anderson, I. I. Shapiro, R. D. Reasenberg, "Venus: Mass, Gravity Field, Atmosphere and Ionosphere as Measured by the Mariner 10 Dual-Frequency Radio System," *Science*, Vol. 183, pp. 1297-1301, 1974b.

Howard, H. T., V. R. Eshleman, D. P. Hinson, A. J. Kliore, G. F. Lindal, R. Woo, M. K. Bird, H. Volland, P. Edenhofer, M. Patzold, and H. Porsche, "Galileo Radio Science Investigations," Vol. 60, pp. 565-590, May 1992.

Hubbard, W. B., and J. D. Anderson, "Possible Flyby Measurements of Galilean Satellite Interior Structure," *Icarus*, Vol. 33, pp. 336-341, 1978.

Hubbard, W. B., W. J. Nellis, A. C. Mitchell, N. C. Holmes, S. S. Limaye, and P. C. McCandless, "Interior Structure of Neptune: Comparison with Uranus," *Science*, Vol. 253, pp. 648-651, 1991.

Janle, P., and E. Erkul, Gravity Studies of the Tharis Area on Mars, Earth, Moon, *Planets* 53 (Netherlands), pp. 217-232, 1991.

Jenkins, J. M., P. G. Steffes, J. Twicken, D. P. Hinson, and G. L. Tyler, "Radio Occultation Studies of the Venus Atmosphere with the Magellan Spacecraft. 2. Results from the October 1991 Experiment," submitted to *Icarus*, 1993.

Jordan, J. F., and J. Lorell, "Mariner 9: An Instrument of Dynamical Science," *Icarus*, Vol. 25, pp. 146-165, 1975.

Kinman, P. W., and S. W. Asmar, "Two-Way Coherent Doppler Error Due to Solar Corona," *TDA Progress Report*, Vol. 42-95, Jet Propulsion Laboratory, Pasadena, California, 1988.

Kinman, P. W., "Doppler Tracking of Planetary Spacecraft," *IEEE Transactions on Microwave Theory and Techniques*, Vol. 40, No. 6, June 1992.

Kliore, A., D. L. Cain, T. W. Hamilton, *Determination of Some Physical Properties of the Atmosphere of Mars from Changes in the Doppler Signal of a Spacecraft on an Earth-Occultation Trajectory*, Technical Report 32-674, Jet Propulsion Laboratory, Pasadena, California, 1964.

Kliore, A., D. L. Cain, G. S. Levy, V. R. Eshleman, G. Fjeldbo, and F. D. Drake, "Occultation Experiment: Results of the First Direct Measurement of Mars' Atmosphere and Ionosphere," *Science*, Vol. 149, pp. 1243-1248, 1965.

Kliore, A., G. S. Levy, D. L. Cain, G. Fjeldbo, and S. I. Rasool, "Atmosphere and Ionosphere of Venus from the Mariner V S-Band Radio Occultation Measurement," *Science*, Vol. 158, pp. 1683-1688, 1967.

Kliore, A. J., and D. L. Cain, "Mariner V and the Radius of Venus," *Journal of Atmospheric Science*, Vol. 25, pp. 549-554, 1968.

Kliore, A., G. Fjeldbo, B. L. Seidel, S. I. Rasool, "Mariners 6 and 7: Radio Occultation Measurements of the Atmosphere of Mars," *Science*, Vol. 166, pp. 1393-1397, 1969.

Kliore, A., "Current Methods of Radio Occultation Data Inversion in Mathematics of Profile Inversion," NASA, TM X-62, 150, edited by L. Colin, pp. 312-316, National Aeronautics and Space Administration, Washington, D. C., 1972.

Kliore, A. J., D. L. Cain, G. Fjeldbo, B. L. Seidel, M. J. Sykes, and S. I. Rasool, "The Atmosphere of Mars from Mariner 9 Radio Occultation Measurements," *Icarus*, Vol. 17, pp. 484-516, 1972.

Kliore, A. J., G. Fjeldbo, B. L. Seidel, M. J. Sykes, and P. M. Woiceshyn, "S Band Radio Occultation Measurements of the Atmosphere and Topography of Mars with Mariner 9: Extended Mission Coverage of Polar and Intermediate Latitudes," *Journal of Geophysical Research*, Vol. 78, pp. 4331-4351, 1973.

Kliore, A. J., G. Fjeldbo, B. L. Seidel, D. N. Sweetnam, T. T. Sesplaukis, P. M. Woiceshyn, S. I. Rasool, "The Atmosphere of Io from Pioneer 10 Radio Occultation Measurements," *Icarus*, Vol. 24, pp. 407-410, 1975.

Kliore, A. J., and P. M. Woiceshyn, "Structure of the Atmosphere of Jupiter from Pioneer 10 and 11 Radio Occultation Measurements," *Jupiter*, edited by T. Gehrels, pp. 216-237, Univ. of Arizona Press, Tucson, Arizona, 1976.

Kliore, A. J., C. Elachi, I. R. Patel, and J. B. Cimino, "Liquid Content of the Lower Clouds of Venus as Determined from Mariner 10 Radio Occultation," *Icarus*, Vol. 37, pp. 51-72, 1979a.

Kliore, A. J., R. Woo, J. W. Armstrong, I. R. Patel, and T. A. Croft, "The Polar Ionosphere of Venus Near the Terminator from Early Pioneer Venus Orbiter Radio Occultations," *Science*, Vol. 203, pp. 765-768, 1979b.

Kliore, A. J., I. R. Patel, A. F. Nagy, T. E. Cravens, and T. I. Gombosi, "Initial Observations of the Nightside Ionosphere of Venus from Pioneer Venus Orbiter Radio Occultations," *Science*, Vol. 205, pp. 99-102, 1979c.

Kliore, A. J., G. F. Lindal, I. R. Patel, D. N. Sweetnam, H. B. Holtz, and T. R. McDonough, "Vertical Structure of the Ionosphere and Upper Neutral Atmosphere of Saturn from the Pioneer Radio Occultation," *Science*, Vol. 207, pp. 446-449, 1980a.

Kliore, A. J., I. R. Patel, G. F. Lindal, D. N. Sweetnam, H. B. Holtz, J. H. Waite, Jr., and T. R. McDonough, "Structure of the Ionosphere and Atmosphere of Saturn from Pioneer 11 Saturn Radio Occultation," *Journal Geophysical Research*, Vol. 85, pp. 5857-5870, 1980b.

Kliore, A. J., and I. R. Patel, "Vertical Structure of the Atmosphere of Venus from Pioneer Venus Orbiter Radio Occultations," *Journal of Geophysical Research*, Vol. 85, pp. 7957-7962, 1980.

Kliore, A. J., J. G. Luhmann, and M.H.G. Zhang, "The Effect of Solar Cycle on the Maintenance of the Nightside Ionosphere of Venus," *Journal of Geophysical Research*, Vol. 96, No. 11, pp. 11065-11071, 1991.

Kliore, A. J., J. G. Luhmann, "Solar Cycle Effects on the Structure of the Electron Density Profiles of the Dayside Ionosphere of Venus," *Journal of Geophysical Research*, Vol. 85, pp. 21281-21289, 1991.

Kliore, A. J., J. D. Anderson, S. W. Asmar, B. Bertotti, N. Borderies, F. M. Flaser, R. G. French, C. L. Hamilton, L. Iess, E. A. Marouf, A. F. Nagy, M. Tinto, and H. Wahlquist, *Investigation Description and Science Requirement Document: Cassini Radio Science Team*, internal document, Jet Propulsion Laboratory, Pasadena, California, 1992.

Koehler, R. L., "Radio Propagation Measurements of Pulsed Plasma Streams from the Sun Using Pioneer Spacecraft," *Journal of Geophysical Research*, Vol. 73, pp. 4883-4894, 1968.

Konopoliv, A. S., N. J. Borderies, P. W. Chodas, E. J. Christensen, W. L. Sjogren, and B. G. Williams, "Venus Gravity and Topography: 60th Degree and Order Model," *Geophysical Research Letters*, in press, 1993.

Krisher, T. P., J. D. Anderson, J. K. Campbell, "Test of the Gravitational Redshift Effects at Saturn," *Physical Review Letters*, Vol. 64, No. 12, March 19, 1990.

Krisher, T. P., J. D. Anderson, D. D. Morabito, S. W. Asmar, S. E. Borutzki, M. L. Delitsky, A. C. Densmore, P. M. Eshe, G. D. Lewis, M. J. Maurer, D. L. Gresh, P. A. Rosen, D. C. Roth, Y. H. Son, T. R. Spilker, D. N. Sweetnam, A. H. Taylor, and G. L. Tyler, "Radio Range Measurements of Coronal Electron Densities at 13 and 3.6 Centimeter Wavelengths During the 1988 Solar Conjunction of Voyager 2," *Astrophysical Journal*, Vol. 375, pp. L57-L60, 1991a.

Krisher, T. P., J. D. Anderson, and A. H. Taylor, "Voyager 2 Test of the Radar Time-Delay Effect," *Astrophysical Journal*, Vol. 373, pp. 665-670, 1991b.

Krisher, T. P., D. D. Morabito, J. D. Anderson, "The Galileo Solar Redshift Experiment," *Physical Review Letters*, Vol. 70, No. 15, April 12, 1993.

Kursinski, E. R., and S. W. Asmar, "Radio Science Ground Data System for the Voyager Neptune Encounter, I," *TDA Progress Report*, Vol. 42-105, Jet Propulsion Laboratory, Pasadena, California, 15 May 1991.

Levy, G. S., T. Sato, B. L. Seidel, C. T. Stelzried, J. E. Ohlson, and W. V. T. Rusch, "Pioneer 6: Measurement of Transient Faraday Rotation Phenomena Observed During Solar Occultation," *Science*, Vol. 166, pp. 596-598, 1969.

Levy, G. S., D. W. Green, H. N. Royden, G. E. Wood and L. L. Tyler, "Dispersive Doppler Measurement of the Electron Content of the Torus of Io," *Journal of Geophysical Research*, Vol. 86A, pp. 8467-8470, 1981.

Lindal, G. F., H. B. Hotz, D. N. Sweetnam, Z. Shippony, J. P. Brenkle, G. V. Hartsell, R. T. Spear, and W. H. Michael, Jr., "Viking Radio Occultation Measurements of the Atmosphere and Topography of Mars: Data Acquired During 1 Martian Year of Tracking," *Journal of Geophysical Research,* Vol. 84, pp. 8443-8456, 1979.

Lindal, G. F., G. E. Wood, G. S. Levy, J. D. Anderson, D. N. Sweetnam, H. B. Hotz, B. J. Buckles, D. P. Holmes, P. E. Doms, V. R. Eshleman, G. L. Tyler and T. A. Croft, "The Atmosphere of Jupiter: An Analysis of the Voyager Radio Occultation Measurements," *Journal of Geophysical Research,* Vol. 86A, pp. 8721-8727, September, 1981.

Lindal, G. F., G. E. Wood, H. B. Hotz, D. N. Sweetnam, V. R. Eshleman, and G. L. Tyler, "The Atmosphere of Titan: An Analysis of the Voyager 1 Radio Occultation Measurements," *Icarus,* Vol. 53, pp. 348-363, 1983.

Lindal, G. F., D. N. Sweetnam and V. R. Eshleman, "The Atmosphere of Saturn: An Analysis of the Voyager Radio Occultation Measurements," *The Astronomical Journal,* Vol. 90, pp. 1136-1146, June 1985.

Lindal, G. F., J. R. Lyons, D. N. Sweetnam, V. R. Eshleman, D. P. Hinson and G. L. Tyler, "The Atmosphere of Uranus: Results of Radio Occultation Measurements," *Journal of Geophysical Research,* Vol. 92, pp. 14987-15001, December 1987.

Lindal, G. F., "Atmosphere of Neptune," *The Astronomical Journal,* Vol. 103, pp. 967-982, 1992.

Martin, J. M., G. L. Tyler, V. R. Eshleman, G. E. Wood, and G. F. Lindal, "A Search for the Radio Occultation Flash at Jupiter," *Journal of Geophysical Research,* Vol. 86A, pp. 8729-8732, 1981.

Marouf, E. A., and G. L. Tyler, "Microwave Edge Diffraction by Features in Saturn's Rings: Observations with Voyager 1," *Science,* Vol. 217, pp. 243-245, 1982.

Marouf, E. A., G. L. Tyler, H. A. Zebker, R. A. Simpson and V. R. Eshleman, "Particle Size Distributions in Saturn's Rings at Wavelengths of 3.6 and 13 cm from Voyager 1 Radio Occultation," *Icarus,* Vol. 54, pp. 189-211, 1983.

Marouf, E. A., and G. L. Tyler, "Radio Occultation by Saturn's Rings: Observations of Structure and Particle Size with Voyager 1," *Advances in Space Research,* Vol. 5, No. 8, pp. 117-120, 1985.

Marouf, E. A., and G. L. Tyler, "Detection of Two Satellites in the Cassini Division of Saturn's Rings," *Nature,* Vol. 323, pp. 31-35, September 1986.

Marouf, E. A., G. L. Tyler, and P. A. Rosen, "Profiling Saturn's Rings by Radio Occultation," *Icarus*, Vol. 68, pp. 120-166, October, 1986.

McNamee, J. B., N. Borderies, and W. L. Sjogren, "Venus: Global Gravity and Topography," submitted for publication in the *Journal of Geophysical Research*, 1992.

Michelson, P. F., Price, J. C., and Taber, R. C., "Resonant Mass Detectors of Gravitational Radiation," *Science*, Vol. 237, p. 150, 1987.

Mottinger, N. A., W. L. Sjogren, and B. G. Bills, "Venus Gravity: A Harmonic Analysis and Geophysical Implications," *Journal of Geophysical Research*, Vol. 90 (supplement), pp. C739-C756, 1985.

Muhleman, D. O., J. D. Anderson, P. B. Esposito, and W. L. Martin, "Radio Propagation Measurements of the Solar Corona and Gravitational Field: Applications to Mariner 6 and 7," in *Proceedings of The Conference on Experimental Tests of Gravitation Theories*, Tech. Memo. 33-499, edited by R. W. Davies, pp. 92-104, Jet Propulsion Laboratory, Pasadena, California, 1971.

Muhleman, D. O., P. B. Esposito, and J. D. Anderson, "The Electron Density Profile of the Outer Corona and the Interplanetary Medium from Mariner-6 and Mariner-7 Time-Delay Measurements," *Astrophysical Journal*, Vol. 211, pp. 943-957, 1977.

Muhleman, D. O., and J. D. Anderson, "Solar Wind Electron Densities from Viking Dual-Frequency Radio Measurements, *Astrophysical Journal*, Vol. 247, pp. 1093-1101, 1981.

Muller, P. M., and W. I. Sjogren, "Mascons: Lunar Mass Concentrations," *Science*, Vol. 161, pp. 680-684, 1968.

Nerem, R. S., "An Improved Gravity Model for Venus Using Tracking Data from Pioneer Venus Orbiter," EOS Transactions, *American Geophysical Union*, Vol. 72, no.17, pp. 174-175, 1991.

Nerem, R. S., B. G. Bills, and J. B. McNamee, "A High Resolution Gravity Model for Venus: GVM-1," *Geophysical Research Letters*, in press, 1993.

Null, G. W., J. D. Anderson, and S. K. Wong, "Gravity Field of Jupiter from Pioneer 11 Tracking Data," *Science*, Vol. 188, pp. 476-477, 1975.

Null, G. W., "Gravity Field of Jupiter and Its Satellites from Pioneer 10 and Pioneer 11 Tracking Data," *The Astronomical Journal*, Vol. 81, pp. 1153-1161, 1976.

Null, G. W., E. L. Lau, E. D. Biller, and J. D. Anderson, "Saturn Gravity Results obtained for Pioneer 11 Tracking Data and Earth-Bound Saturn Satellite Data," *The Astronomical Journal*, Vol. 86, pp. 456-468, 1981.

Ohlson, J. E., G. S. Levy, and C. T. Stelzried, "A tracking Polarimeter for Measuring Solar and Ionospheric Faraday Rotation of Signals from Deep Space Probes," *IEEE Transactions on Instrumentation and Measurement IM*, Vol. 23, pp. 167-177, 1974.

Pätzold, M., M. K. Bird, H. Volland, G. S. Levy, B. L. Seidel, C. T Stelzreid, "The Mean Coronal Magnetic Field Determined from Helios Faraday Rotation Measurements," *Solar Physics*, Vol. 109, pp. 91-105, 1987.

Pätzold, M., *The Dynamics of the Giotto Spacecraft in the Inner Dust Coma of Comet P/Halley as Determined From the Giotto Radio-Science Experiment*, doctoral dissertation, University of Bonn, Germany, May 1990.

Pätzold, M., M.K. Bird, and H. Volland, "Giotto-Halley encounter: When was the large nutation generated?" *Astronomy and Astrophysics*, Vol. 244, pp. L17-L20, 1991.

Pätzold, M., M. K. Bird, H. Volland, P. Edenhofer, and H. Buschert, "Dynamics of the Giotto Spacecraft in the Inner Dust Coma of Comet P/Halley; Part I: Observations," *Z. Flugwiss. Weltraumforsch.*, Vol. 15, pp. 89-96, 1991.

Pätzold, M., M. K. Bird, H. Volland, P. Edenhofer, and H. Buschert, "Dynamics of the Giotto Spacecraft in the Inner Dust Coma of Comet P/Halley; Part II: Interpretations," *Z. Flugwiss. Weltraumforsch.*, Vol. 15, pp. 159-164, 1991.

Pätzold, M., M. K. Bird, H. Volland, S. W. Asmar, J. P. Brenkle, "Coronal Sounding with Ulysses: Preliminary Results from the First Solar Conjunction," Solar Wind Seven Proceedings in *Advances in Space Research*, 1992.

Pätzold, M., H. Porsche, P. Edenhofer, M. K. Bird, and H. Volland, "Giotto Radio-Science Experiment: Expected Drag Deceleration and Spacecraft Attitude Perturbations During the Encounter with Comet P/Grigg-Skjellerup in July 1992," *Astronomy and Astrophysics*, Vol. 259, pp. L15-L18, 1992.

Pätzold, M., P. Edenhofer, M. K. Bird, and H. Volland, "The Giotto Encounter with Comet Grigg-Skjellerup: First Results From the Giotto Radio-Science Experiment," *Astronomy and Astrophysics*, Vol. 268, pp. L13-L16, 1993.

Pätzold, M., M. K. Bird, and P. Edenhofer, "The Change of Giotto's Dynamical State During the P/Grigg-Skjellerup Flyby Caused by Dust Particle Impacts," submitted to *Journal of Geophysical Research*, 1993.

Reasenberg, R. D., and I. I. Shapiro, "Solar System Tests of General Relativity, in Experimental Gravitation," Acad. Naz. dei Lincei, Roma, Italy, 1977.

Reasenberg, R. D., I. I. Shapiro, P. E. MacNeil, R. B. Goldstein, J. C. Briedenthal, J. P. Brenkle, D. L. Cain, T. M. Kaufman, T. A. Komarek and A. I. Zygielbaum, "Viking Relativity Experiment: Verification of Signal Retardation by Solar Gravity," *Astrophysical Journal* Vol. 234, pp. L219-L221, 1979.

Reid, M. S., R. C. Clauss, D. A. Bathker, and C. T. Stelzried, "Low-Noise Microwave Receiving Systems in a Worldwide Network of Large Antennas," *Proceedings of the IEEE*, Vol. 61, pp. 1330-1335, 1973.

Riley, A. L., D. Antsos, J. Armstrong, P. Kinman, H. Wahlquist, B. Bertotti, G. Comoretto, B. Pernice, G. Carnicella, R. Giordani, S. Spazio, "Cassini Ka-Band Precision Doppler and Enhanced Telecommunications System Study," sponsored by NASA and the Italian Space Agency, 1990.

Rockwell, R. S., "An Empirical Spectral Bandwidth Model for Superior Conjunction," *DSN Progress Report*, Vol. 42-43, Jet Propulsion Laboratory, Pasadena, California, pp. 215-223, 1978.

Rosborough, G. W., and F. G. Lemoine, Sensitivity Studies of Mars Orbiters for Mars Gravity Recovery, *Journal of the Astronautical Sciences*, Vol. 39, pp. 327-357, 1991.

Rosen, P. A., and J. J. Lissauer, "The Titan -1:0 Nodal Bending Wave in Saturn's Ring C," *Science*, Vol. 241, pp. 690-694, 1988.

Rusch, W. V. T., and C. T. Stelzried, "Net-field Polarization in a Magnetically Biased Plasma," *Radio Science*, Vol. 7, pp. 1131-1141, 1972.

Shapiro, I. I., R. D. Reasenberg, P. E. MacNeil, R. B. Goldstein, J. P. Brenkle, D. L. Cain, T. Komarek, A. I. Zygielbaum, W. F. Cuddihy, and W. H. Michael, Jr., "The Viking Relativity Experiment," *Journal of Geophysical Research*, Vol. 82, pp. 4329-4334, 1977.

Showalter, M. R., J. N. Cuzzi, E. A. Marouf and L. W. Esposito, "Satellite 'Wakes' and the Orbit of the Encke Gap Moonlet," *Icarus*, Vol. 66, pp. 297-323, 1986.

Showalter, M. R., "Visual Detection of 1981 S13, Saturn's Eighteenth Satellite, and Its Role in the Encke Gap," *Nature*, Vol. 351, pp. 709-713, 1991.

Simpson, R. A., and G. L. Tyler, "Viking Bistatic Radar Experiment: Summary of First-Order Results Emphasizing North Polar Data," *Icarus*, Vol. 46, pp. 361-389, 1981.

Simpson, R. A., G. L. Tyler and J. B. Holberg, "Saturn's Pole: Geometric Correction Based on Voyager UVS and Radio Occultations," *The Astronomical Journal*, Vol. 88, pp. 1531-1536, 1983.

Simpson, R. A., G. L. Tyler, E. A. Marouf, H. A. Zebker and V. R. Eshleman, "Saturn's Rings: Voyager 1 Radio Occultation Experiment Results," *IEEE Transactions on Geoscience Electronics and Remote Sensing*, Vol. GE-22, pp. 656-665, 1984.

Sjogren, W. L., J. D. Anderson, R. J. Phillips, and D. W. Trask, "Gravity Fields," *IEEE Transactions on Geoscience Electronics*, Vol. GE-14, No. 3, pp. 172-183, 1976.

Sjogren, W. L., "Mars Gravity: High-Resolution Results from Viking Orbiter 2," *Science*, Vol. 203, pp. 1006-1007, 1979.

Sjogren, W. L., and R. N. Wimberly, "Mars: Hellas Planitia Gravity Analysis," *Icarus*, Vol. 45, pp. 331-338, 1981.

Sjogren, W. L., B. G. Bills, P. W. Birkeland, P. B. Esposito, A. R. Konopliv, N. A. Mottinger, S. J. Ritke, and R. J. Phillips, "Venus Gravity Anomalies and the Correlations with Topography," *Journal of Geophysical Research*, Vol. 88, pp. 1119-1128, 1983.

Sjogren, W. L., B. G. Bills, and N. A. Mottinger, "Venus: Ishtar Gravity Anomaly," *Geophysical Research Letters*, Vol. 11, pp. 489-491, 1984.

Sjogren, W. L., J. D. Anderson, R. J. Phillips, and D. W. Trask, "Gravity Fields," *IEEE Trans. Geomag. Elect.*, GE-14, pp. 172-183, 1986.

Smith, D. E., F. J. Lerch, R. S. Nerem, M. T. Zuber, G. B. Patel, S. K. Fricke, and F. G. Lemoine, "An Improved Gravity Model for Mars: Goddard Mars Model -1 (GMM-1)," *Journal of Geophysical Research*, in press, 1993.

Smith E. K., and R. E. Edelson, "Radio Propagation Through Solar and Other Extraterrestrial Ionized Media," Publication 79-117, Jet Propulsion Laboratory, California Institute of Technology, Pasadena, California, January 1980.

Smreker, S. E., and R. J. Phillips, "Venusian Highlands: Geoid to Topography Ratios and Their Implications," *Earth Planet. Science Lett.*, Vol. 107 (Netherlands), pp. 582-597, 1991.

Spradlin, G. L., "DSN Tracking System, Mark III-79," *DSN Progress Report* 42-56, pp.7-25. Jet Propulsion Laboratory, Pasadena, Calif., 1980.

Stelzried, C. T., "A Faraday Rotation Measurement of a 13-cm Signal in the Solar Corona," Technical Report 32-1401, 83 pp., Jet Propulsion Laboratory, Pasadena, Calif., 1970.

Stelzried, C. T., G. S. Levy, T. Sato, W. V. T. Rusch, J. E. Ohlson, K. H. Schatten and J. M. Wilcox, "The Quasi-Stationary Coronal Magnetic Field and Electron Density as Determined from a Faraday Rotation Experiment," *Solar Physics*, Vol. 14, pp. 440-456, 1970.

Steffes, P. G., J. M. Jenkins, G. L. Tyler, J. Twicken, R. S. Austin, and S. W. Asmar, "Preliminary Results from the October 1991 Magellan Radio Occultation Experiment," *Bulletin of the American Astronomical Society*, Vol. 24, p. 1003, October 1992.

Steffes, P. G., J. M. Jenkins, R. S. Austin, S. W. Asmar, D. T. Lyons, E. H. Seale, G. L. Tyler, "Radio Occultation Studies of the Venus Atmosphere With the Magellan Spacecraft, 1. Experiment Description and Performance," submitted to *Icarus*, February 1993.

Thorne, K. S., and V. B. Braginsky,"Gravitational-Wave Bursts from the Nuclei of Distant Galaxies and Quasars: Proposal for Detection Using Doppler Tracking of Interplanetary Spacecraft," *Astrophysical Journal*, Vol. 204, L1-L6, 1976.

Thorne, K. S., "Gravitational Radiation," *In 300 Years of Gravitation*, eds. S. W. Hawking and W. Israel, Cambridge, Cambridge University Press, 1987.

Thorne, K. S., "Sources of Gravitational Waves and Prospects for Their Detection," Caltech preprint GRP-234, California Institute of Technology, Pasadena, California, 1991.

Tyler, G. L., J. P. Brenkle, T. A. Komarek, A. I. Zygielbaum, "The Viking Solar Corona Experiment," *Journal of Geophysical Research*, Vol. 82, pp. 4335-4340, 1977.

Tyler, G. L., V. R. Eshleman, J. D. Anderson, G. S. Levy, G. F. Lindal, G. E. Wood and T. A. Croft, "Radio Science Investigation of the Saturn System with Voyager 1: Preliminary Results," *Science*, Vol. 212, pp. 201-206, 1981.

Tyler, G. L., E. A. Marouf and G. E. Wood, "Radio Occultation of Jupiter's Rings: Bounds on Optical Depth and Particle Size," *Journal of Geophysical Research*, Vol. 86A, pp. 8699-8703, 1981.

Tyler, G. L., V. R. Eshleman, J. D. Anderson, G. S. Levy, G. F. Lindal, G. E. Wood and T. A. Croft, "Radio Science with Voyager 2 at Saturn: Atmosphere and Ionosphere and the Masses of Mimas, Tethys, and Lapetus," *Science*, Vol. 215, pp. 553-558, 1982.

Tyler, G. L., E. A. Marouf, R. A. Simpson, H. A. Zebker and V. R. Eshleman, "The Microwave Opacity of Saturn's Rings at Wavelengths of 3.6 and 13 cm from Voyager 1 Radio Occultation," *Icarus*, Vol. 54, pp. 160-188, 1983.

Tyler, G. L., D. N. Sweetnam, J. D. Anderson, J. K. Campbell, V. R. Eshleman, D. P. Hinson, G. S. Levy, G. F. Lindal, E. A. Marouf and R. A. Simpson, "Voyager 2 Radio Science Observations of the Uranian System: Atmosphere, Rings, and Satellites," *Science*, Vol. 233, pp. 79-84, 1986.

Tyler, G. L., "Radio Propagation Experiments in the Outer Solar System with Voyager," *Proceedings of the IEEE*, Vol. 75, no. 10, 1987.

Tyler, G. L., D. N. Sweetnam, J. D. Anderson, S. E. Borutzki, J.K. Campbell, V. R. Eshleman, D. L. Gresh, E. M. Gurrola, D. P. Hinson, N. Kawashima, E. R. Kursinski, G. S. Levy, G. F. Lindal, J. R. Lyons, E. A. Marouf, and P. A. Rosen, "Observations of Neptune and Triton," *Science*, Vol. 246, pp. 1466-1473, 1989.

Tyler, G. L., G. Balmino, D. P. Hinson, W. L. Sjogren, D. E. Smith, R. Woo, S. W. Asmar, M. J. Connally, C. L. Hamilton, R. A. Simpson, "Radio Science Investigations with Mars Observer," *Journal of Geophysical Research*, Vol. 97, pp. 7759-7779, 1992.

Volland, H., M. K. Bird, G. S. Levy, C. T. Stelzried, and B. L. Seidel, "Helios-1 Faraday Rotation Experiment: Results and Interpretations of the Solar Occultations in 1975," *Journal of Geophysical Research*, Vol. 42, pp. 659-672, 1977.

Waff, C. B., "The Road to the Deep Space Network," *IEEE Spectrum*, April 1993.

Woo, R., F. C. Yang, K. W. Yip, and W. B. Kendall, "Measurements of Large-Scale Density Fluctuations in the Solar Wind Using Dual-Frequency Phase Scintillations," *Astrophysical Journal*, Vol. 210, pp. 568-574, 1977.

Woo, R., "Radial Dependence of Solar Wind Properties Deduced from Helios 1/2 and Pioneer 10/11 Radio Scattering Observations," *Astrophysical Journal* Vol. 219, pp. 727-739, 1978.

Woo, R., and J. W. Armstrong, "Spacecraft Radio Scattering Observations of the Power Spectrum of Electron Density Fluctuations in the Solar Wind," *Journal of Geophysical Research*, Vol. 84, pp. 7288-7296, 1979.

Woo, R., J. W. Armstrong, and A. Ishimaru, "Radio Occultation Measurements of Turbulence in The Venus Atmosphere by Pioneer Venus," *Journal of Geophysical Research*, Vol. 85, pp. 8031-8038, 1980.

Woo, R., and J.W. Armstrong, "Measurements of a Solar Flare-Generated Shock Wave at 13.1 R_0," *Nature*, 292, pp. 608-610, 1981.

Woo, R., J. W. Armstrong, N.R. Sheeley, Jr., R.A. Howard, M.J. Koomen, and D. J. Michels, "Doppler Scintillation Observations of Interplanetary Shocks Within 0.3 AU," *Journal of Geophysical Research,* Vol. 90, pp. 154-162, 1985.

Woo, R., "A Synoptic Study of Doppler Scintillation Transients in the Solar Wind," *Journal of Geophysical Research,* Vol. 93, pp. 3919-3926, 1988.

Woo, R., J. W. Armstrong, R. Schwenn, and F. Tang, "Radio Scintillation Measurements of an Interplanetary Shock at 15.8 R_0," *EOS,* Vol. 71, p. 590, 1990.

Woo, R., and A. J. Kliore, "Magnetization of the Ionosphere of Venus and Mars: Results from Radio Occultation Measurements," *Journal of Geophysical Research,* Vol. 96, pp. 11073-11081, 1991.

Woo, R., and R. Schwenn, "Comparison of Doppler Scintillation and In Situ Spacecraft Plasma Measurements of Interplanetary Disturbances," *Journal of Geophysical Research,* Vol. 96, pp. 21227-21244, 1991.

Woo, R., and J.W. Armstrong, "Observations of Large-Scale Structure in the Inner Heliosphere with Doppler Scintillation Measurements, Solar Wind Seven," *OSPAR Colloquia,* Series 3, pp. 319-322, 1992.

Wahlquist, H. D., J. D. Anderson, F. B. Estabrook, and K. S. Thorne, "Recent JPL Work on Gravity Wave Detection and Solar System Relativity Tests," *Atti dei Convengi Lincei,* Vol. 34, p. 336, 1977.

Wahlquist, H. D., "The Doppler Response to Gravitational Waves from a Binary Star Source," *Gen. Rel. Grav.,* Vol. 19, p. 1101, 1987.

Yakovlev, O. I., "Propagation of Radio Waves in Space," Moscow, USSR, *Science* (in Russian), 1985.

Zebker, H. A., G. L. Tyler, and E. A. Marouf, "On Obtaining the Forward Phase Functions of Saturn Ring Features from Radio Occultation Observations," *Icarus,* Vol. 56, pp. 209-228, 1983.

Zebker, H. A, and G. L. Tyler, "Thickness of Saturn's Rings Inferred from Voyager 1 Observations of Microwave Scatter," *Science,* Vol. 233, pp. 396-398, 1984.

Zebker, H. A., E. A. Marouf, and G. L. Tyler, "Saturn's Rings: Particle Size Distributions for Thin Layer Models," *Icarus,* Vol. 64, pp. 531-548, 1985.

Zuber, M. T., D. E. Smith, F. J. Lerch, R. S. Nerem, G. B. Patel, and S. K. Fricke, "A 40th Degree and Order Gravitational Field Model for Mars," *Lunar Planet. Sci. Conf., XXII*, pp. 1581-1582, 1991.

1. Report No. JPL Pub. 80-93, Rev 1	2. Government Accession No.	3. Recipient's Catalog No.

4. Title and Subtitle The Deep Space Network as an Instrument for Radio Science Research	5. Report Date April 15, 1993
	6. Performing Organization Code

7. Author(s) S. W. Asmar and N. A. Renzetti	8. Performing Organization Report No.

9. Performing Organization Name and Address JET PROPULSION LABORATORY California Institute of Technology 4800 Oak Grove Drive Pasadena, California 91109	10. Work Unit No.
	11. Contract or Grant No. NAS7-918
	13. Type of Report and Period Covered

12. Sponsoring Agency Name and Address NATIONAL AERONAUTICS AND SPACE ADMINISTRATION Washington, D.C. 20546	JPL Publication
	14. Sponsoring Agency Code RE211 BG-314-40-31-30-26 D

15. Supplementary Notes

16. Abstract

Radio science experiments use radio links between spacecraft and sensor instrumentation that is implemented in the Deep Space Network. The deep space communication complexes along with the telecommunications subsystem on board the spacecraft constitute the major elements of the radio science instrumentation. Investigators examine small changes in the phase and/or amplitude of the radio signal propagating from a spacecraft to study the atmospheric and ionospheric structure of planets and satellites, planetary gravitational fields, shapes, masses, planetary rings, ephemerides of planets, solar coraona, magnetic fields, cometary comae, and such aspects of the theory of general relativity as gravitational waves and gravitational redshift.

17. Key Words (Selected by Author(s)) Spacecraft Instrumentation Engineering (General) Geophysics Space Sciences (General)	18. Distribution Statement Unclassified -- Unlimited

19. Security Classif. (of this report) Unclassified	20. Security Classif. (of this page) Unclassified	21. No. of Pages 72	22. Price

JPL 0184 R 9/83